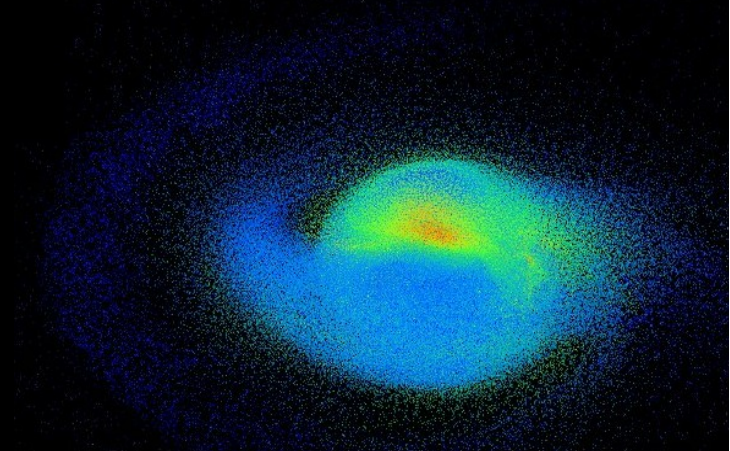
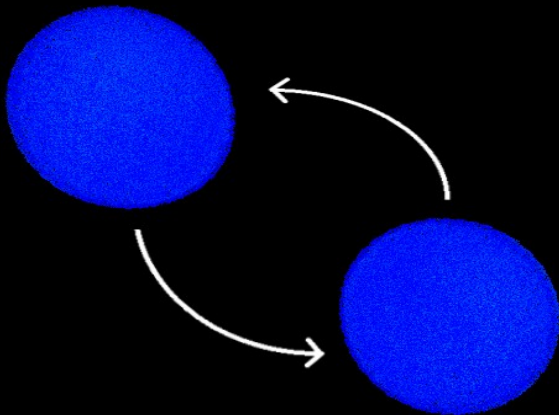


Neutron star mergers and the high-density equation of state

EMMI NQM Seminar, GSI, Darmstadt, 31/01/2018

Andreas Bauswein (Heidelberg Institute for Theoretical Studies)



Outline

- ▶ Introduction and Motivation
- ▶ Some insights from GW170817 and background on NS mergers
- ▶ EoS constraints from NS mergers
 - tidal effects during inspiral
 - postmerger oscillation frequencies
 - GW data analysis aspects
 - radius constraints from collapse behavior
- ▶ Summary and conclusions



KOLLISION VON NEUTRONENSTERNEN

Durchbruch in der Astronomie

 tagesschau

16/10/2017

A break-through in astrophysics

- ▶ GW170817 first unambiguously detected NS merger
- ▶ Multi-messenger observations: gravitational waves, gamma, X-rays, UV, optical, IR, radio

Detection August 17, 2017 by
LIGO-Virgo network

→ GW data analysis

→ follow-up observations -
probably largest coordinated
observing campaign in astronomy
(observations/time)

Announcement October 2017



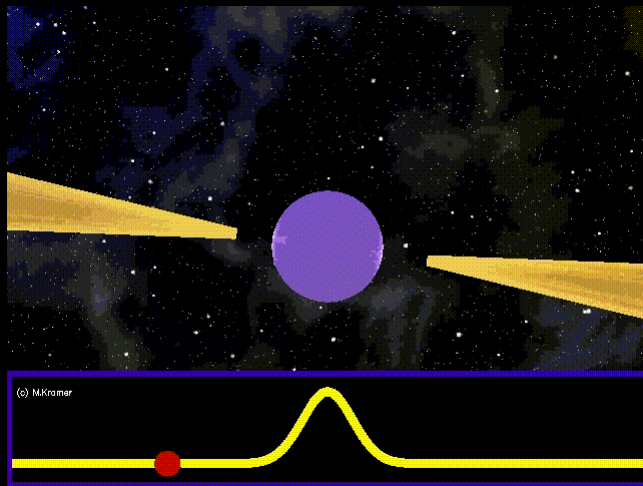
Scientific aspects of NS mergers

- ▶ NS mergers likely progenitors of short gamma-ray bursts (observed since the 70ies)
- ▶ NS mergers as sources of heavy elements forged by the **rapid neutron-capture process***
- ▶ **Electromagnetic transient*** powered by nuclear decays during/after r-process (“kilonova”, “marconova”, ...)
 - UV, optical, IR → targets for triggered or blind searches (time-domain astronomy)
- ▶ Various other types of em counterparts
- ▶ Strong emitters of GWs
 - population properties: masses, rates, ... → stellar astrophysics
 - **EoS of nuclear matter / stellar properties of NSs***
- ▶ ...

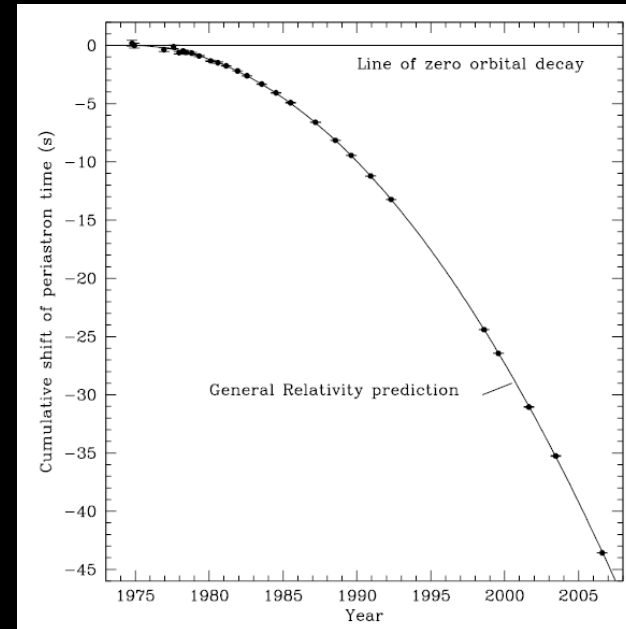
* strong links to scientific work at GSI/FAIR, e.g. CBM, NUSTAR, Theory

Background: NS and NS binaries

- ▶ NSs are end products of massive star evolution
- ▶ Compact stars of typically 1.4 Msun, 10-15 km radius → supra-nuclear densities
- ▶ A few 1000 NSs observed mostly as radio pulsars (~100 million expected in our Galaxy)
- ▶ Many in binary systems with sufficiently “small” orbits (~ 10 known)
- ▶ Decaying orbit measured !! (Nobel prize for Hulse and Taylor)
- ▶ Merger driven by GW emission: point-particle inspiral → dynamical merger phase



M. Kramer



Weisberg et al.

Background: NS and NS binaries

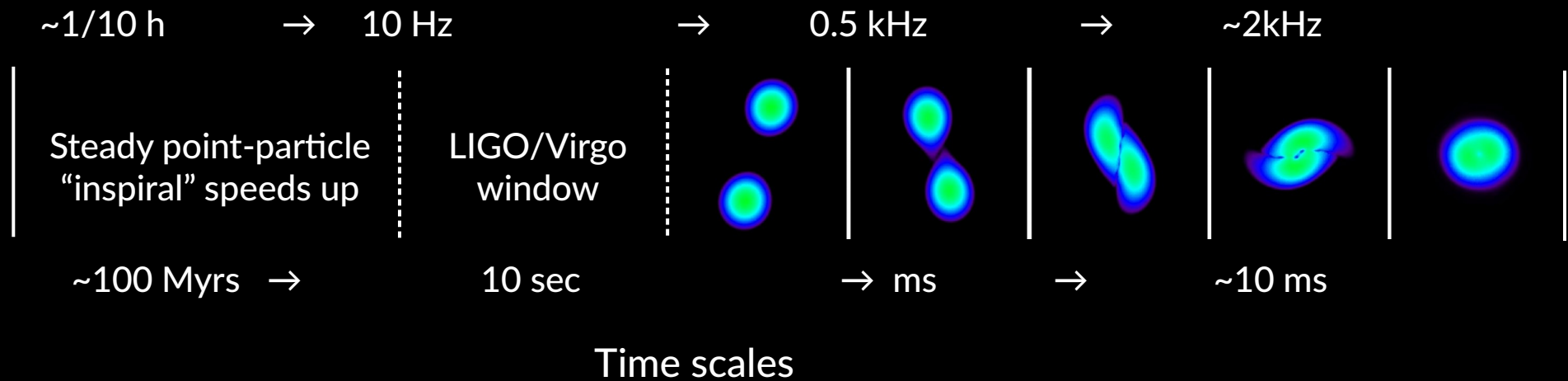
- ▶ Merger driven by GW emission: trajectory = spiral → “inspiral”
point-particle inspiral continuously speeds up → dynamical merger phase

$$E_{orb} = -\frac{1}{2} \frac{M_1 M_2}{a}$$

$$\frac{dE_{orb}}{dt} = -L_{GW}$$

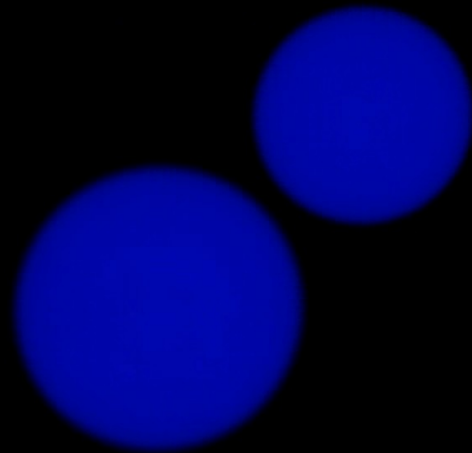
$$f_{orb} = \sqrt{\frac{G(M_1 + M_2)}{4\pi^2 a^3}} = \frac{1}{2} f_{GW}$$

Frequencies

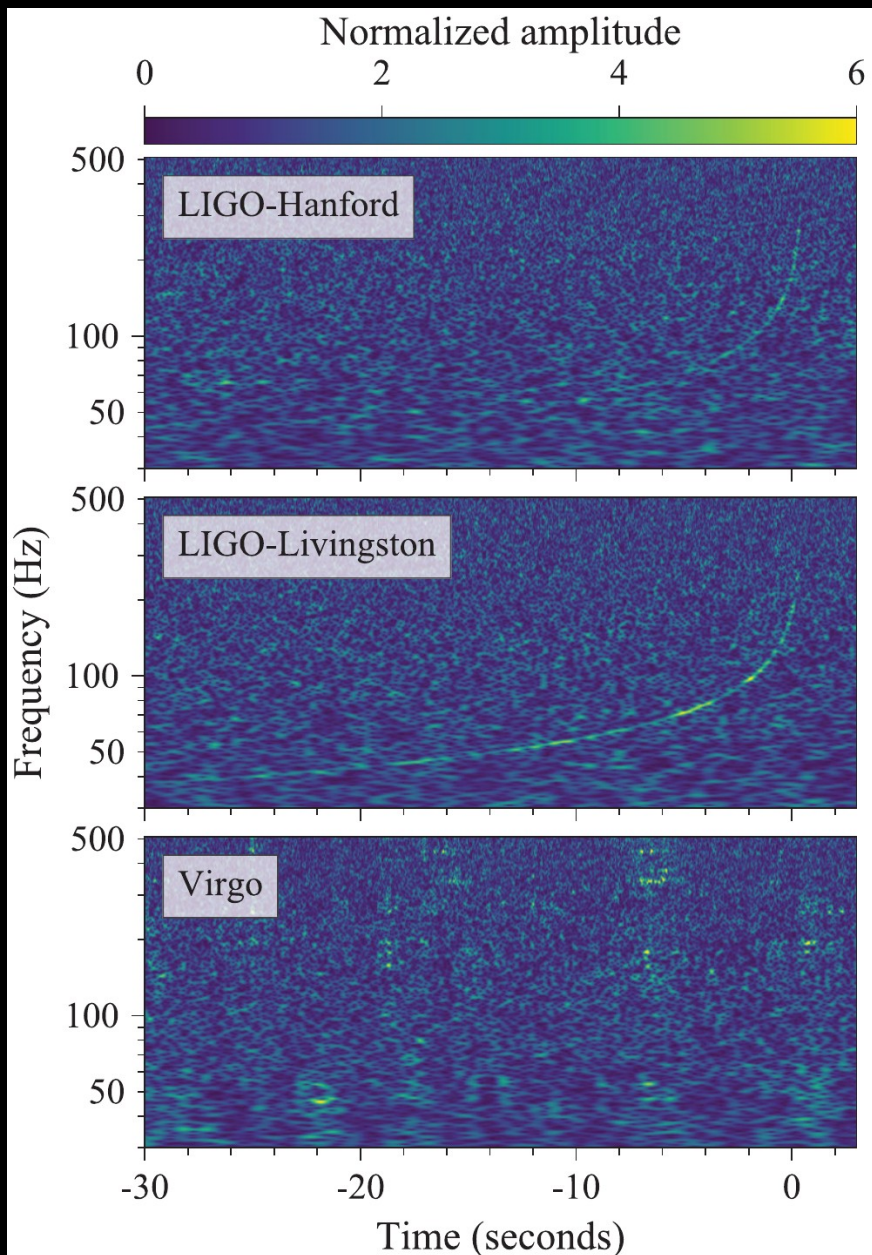




$t = 2.40\text{ms}$



GW170817



| | Low-spin priors ($ \chi \leq 0.05$) |
|--------------------------------------------------------------|----------------------------------------|
| Primary mass m_1 | $1.36\text{--}1.60 M_\odot$ |
| Secondary mass m_2 | $1.17\text{--}1.36 M_\odot$ |
| Chirp mass \mathcal{M} | $1.188^{+0.004}_{-0.002} M_\odot$ |
| Mass ratio m_2/m_1 | $0.7\text{--}1.0$ |
| Total mass m_{tot} | $2.74^{+0.04}_{-0.01} M_\odot$ |
| Radiated energy E_{rad} | $> 0.025 M_\odot c^2$ |
| Luminosity distance D_L | 40^{+8}_{-14} Mpc |
| Viewing angle Θ | $\leq 55^\circ$ |
| Using NGC 4993 location | $\leq 28^\circ$ |
| Combined dimensionless tidal deformability $\tilde{\Lambda}$ | ≤ 800 |
| Dimensionless tidal deformability $\Lambda(1.4M_\odot)$ | ≤ 800 |

Chirp-like signal \rightarrow compact binary merger

Shape reveals masses \rightarrow only compatible with NSs

\rightarrow triggered some follow-up observations

Some insights from GW170817

- ▶ Binary masses measured from “inspiral” (= pre-merger phase with shrinking orbit)
- ▶ Detection at 40 Mpc → rate is presumably high !
- ▶ Note: chirp mass accurately measured
- ▶ Mass ratio only at higher PN order

$$\mathcal{M}_{chirp} = \frac{(M_1 M_2)^{3/5}}{(M_1 + M_2)^{1/5}}$$

$$q = M_1/M_2$$

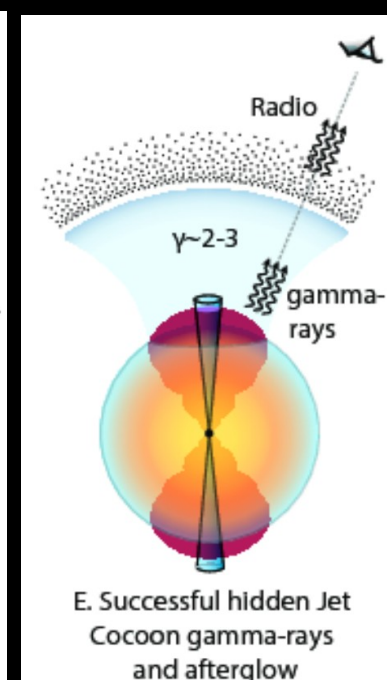
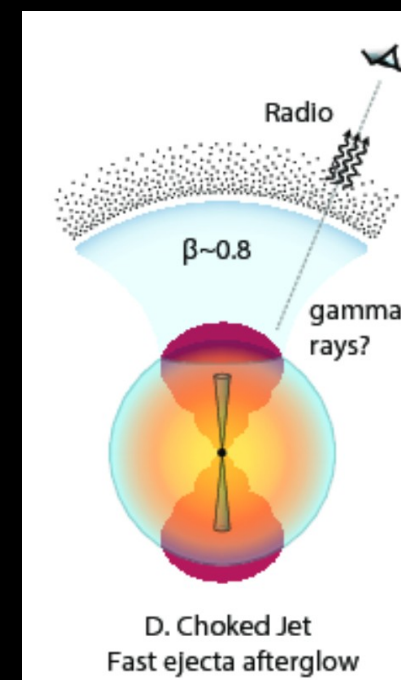
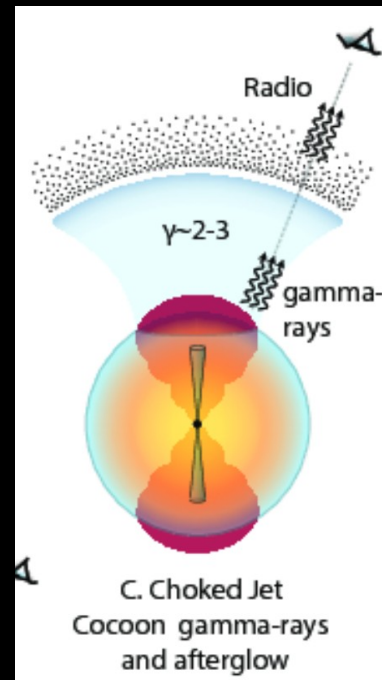
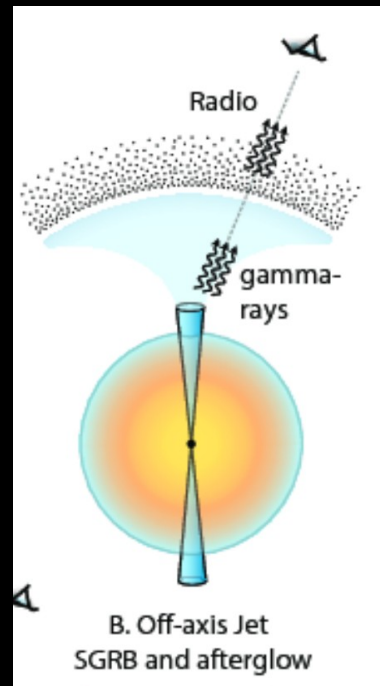
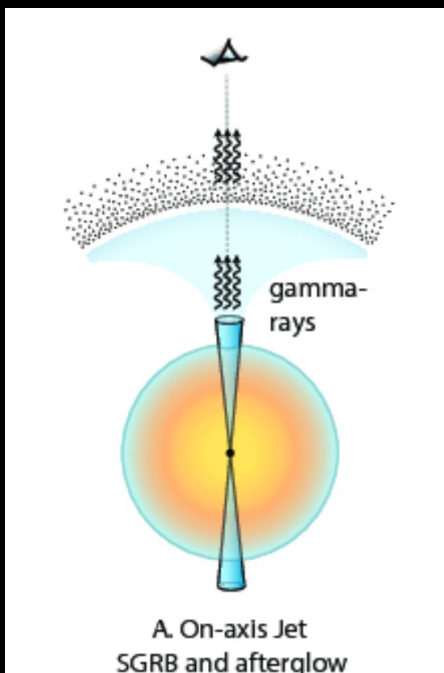
Abbott et al. 2017

| | Low-spin priors ($ \chi \leq 0.05$) | High-spin priors ($ \chi \leq 0.89$) |
|--------------------------------------------------------------|----------------------------------------|-----------------------------------------|
| Primary mass m_1 | 1.36–1.60 M_\odot | 1.36–2.26 M_\odot |
| Secondary mass m_2 | 1.17–1.36 M_\odot | 0.86–1.36 M_\odot |
| Chirp mass \mathcal{M} | 1.188 $^{+0.004}_{-0.002}$ M_\odot | 1.188 $^{+0.004}_{-0.002}$ M_\odot |
| Mass ratio m_2/m_1 | 0.7–1.0 | 0.4–1.0 |
| Total mass m_{tot} | 2.74 $^{+0.04}_{-0.01}$ M_\odot | 2.82 $^{+0.47}_{-0.09}$ M_\odot |
| Radiated energy E_{rad} | $> 0.025 M_\odot c^2$ | $> 0.025 M_\odot c^2$ |
| Luminosity distance D_L | 40 $^{+8}_{-14}$ Mpc | 40 $^{+8}_{-14}$ Mpc |
| Viewing angle Θ | $\leq 55^\circ$ | $\leq 56^\circ$ |
| Using NGC 4993 location | $\leq 28^\circ$ | $\leq 28^\circ$ |
| Combined dimensionless tidal deformability $\tilde{\Lambda}$ | ≤ 800 | ≤ 700 |
| Dimensionless tidal deformability $\Lambda(1.4M_\odot)$ | ≤ 800 | ≤ 1400 |

Some insights from GW170817

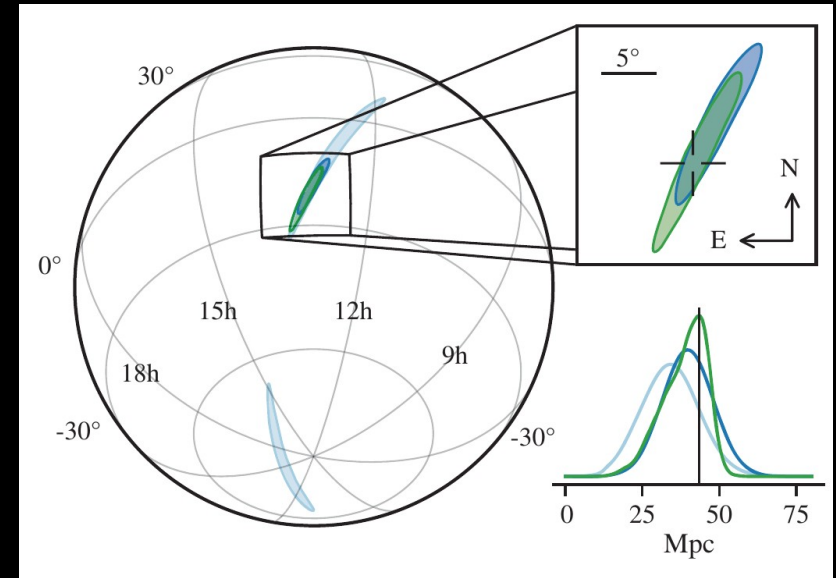
- ▶ Binary masses measured from inspiral
- ▶ Detection at 40 Mpc → rate is presumably high !
- ▶ Gamma-ray burst (?) followed 1.7 sec after GWs – but sub-luminous (by orders of magnitude)
- ▶ X-ray and radio observations several days after merger (on-going)
→ different interpretations (off-axis, cocoon, choked, ...)

Sketches from Mooley et al. 2017



Observations

- ▶ Follow up observation (UV, optical, IR) starting ~ 12 h after merger
- ejecta masses, velocities, opacities
- red and blue component fit data
- spectral features of heavy elements (?)



Abbott et al. 2017

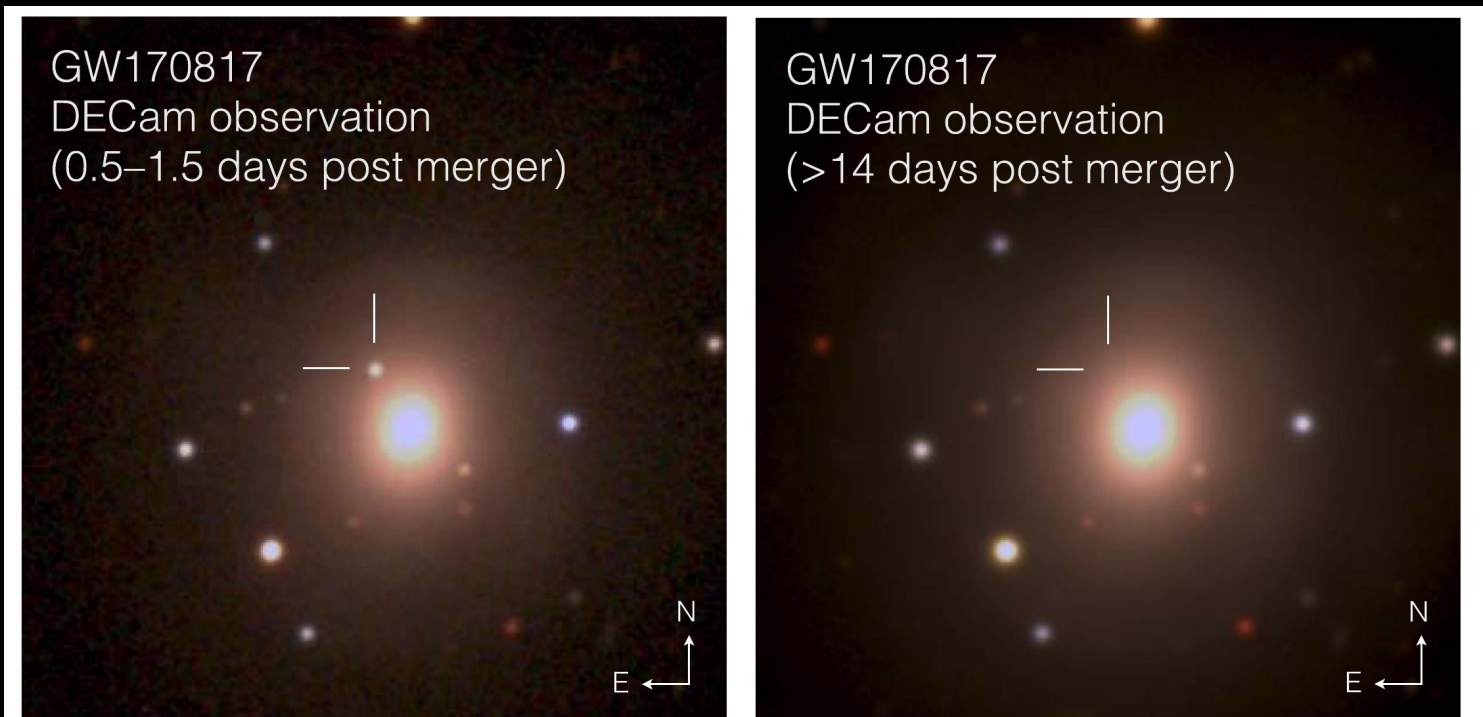
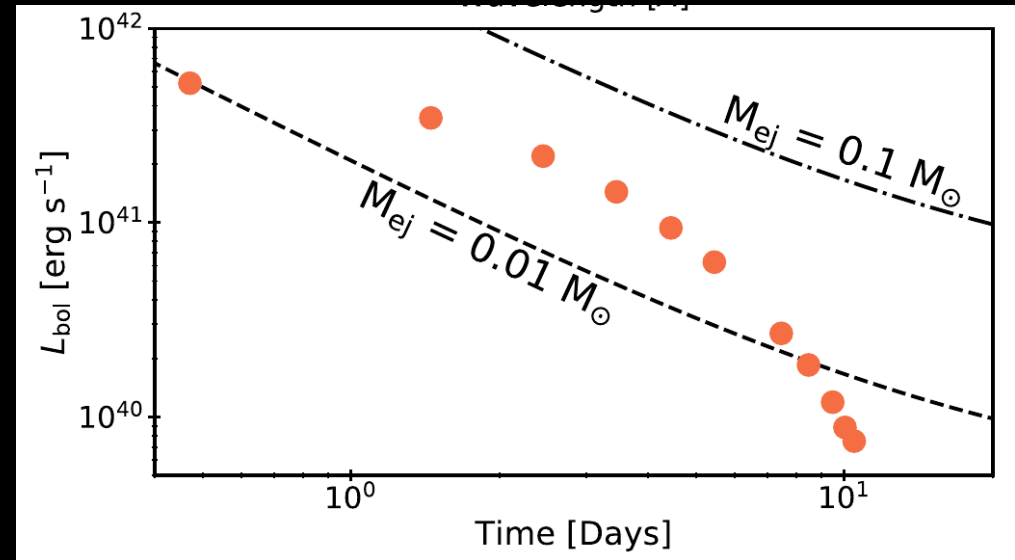
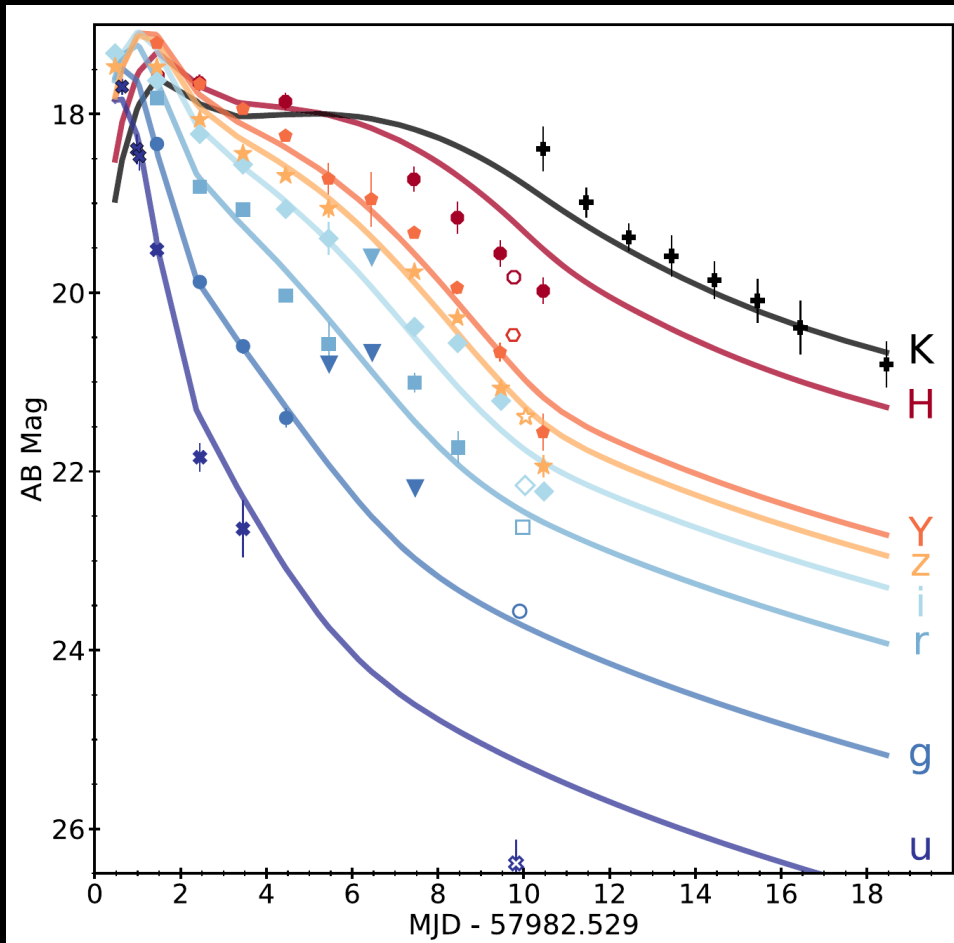


Figure 1. NGC4993 *grz* color composites ($1/5 \times 1/5$). Left: composite of detection images, including the discovery *z* image taken on 2017 August 18 00:05:23 UT and the *g* and *r* images taken 1 day later; the optical counterpart of GW170817 is at R.A., decl. =197.450374, -23.381495 . Right: the same area two weeks later.

Soares-Santos et al 2017

Observations

- ▶ Light curves and derived ejecta masses



Interpreted as multi-component outflow

Fast blue 0.01 M_{sun} + slower red 0.04 M_{sun}

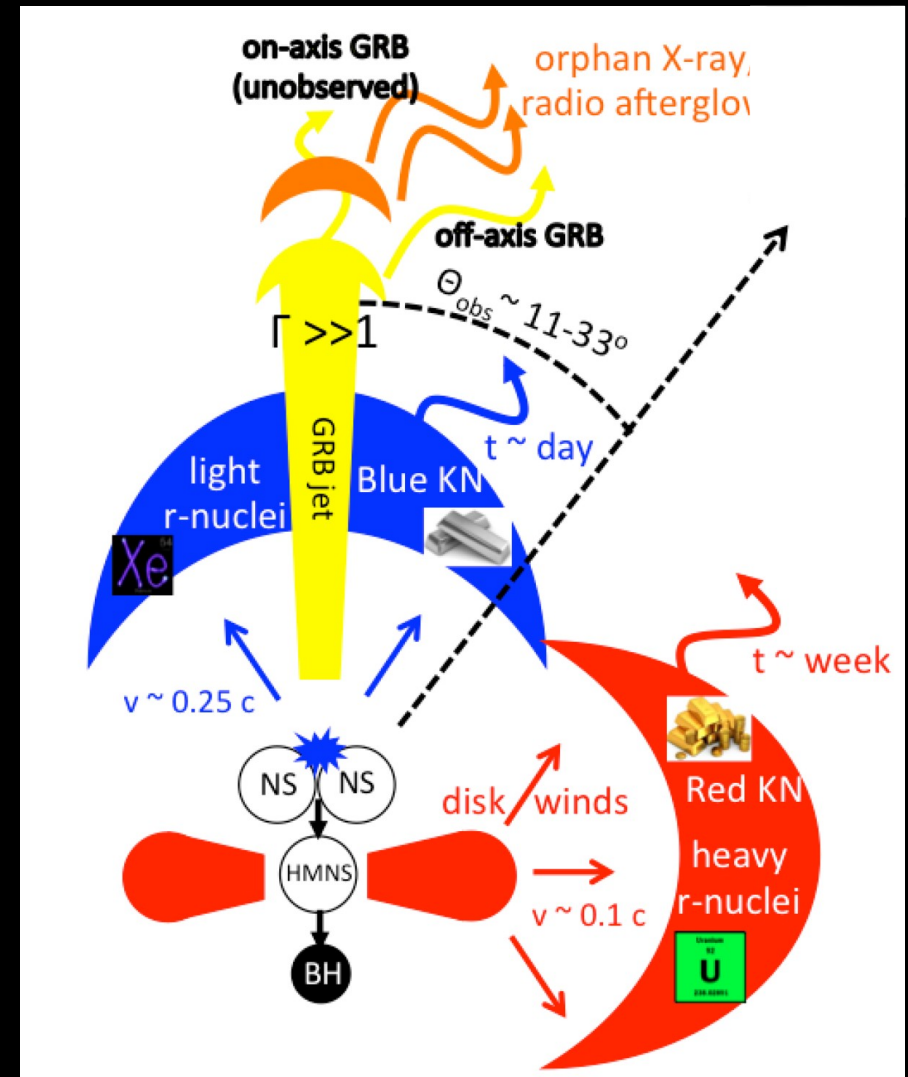
Cowperthwaite et al. 2017 (DECam, Gemini-South, HST observations)

Observations

- ▶ Many IR/opt/UV observations by many groups
- ▶ Different interpretations / modeling
- ▶ Derived total ejecta masses all in the range 0.03 ... 0.05 Msun

Chronock et al. 2017, Levan & Tanvir 2017, Kasliwal et al. 2017, Coulter et al. 2017, Allam et al. 2017, Yang et al. 2017, Arcavi et al. 2017, Kilpatrick et al. 2017, McCully et al. 2017, Pian et al. 2017, Arcavi et al. 2017, Evans et al. 2017, Drout et al. 2017 Lipunov et al. 2017, Cowperthwaite et al. 2017, Smartt et al. 2017, Shappee et al. 2017, Nicholl et al. 2017, Kasen et al. 2017, Tanaka et al. 2017,

.....



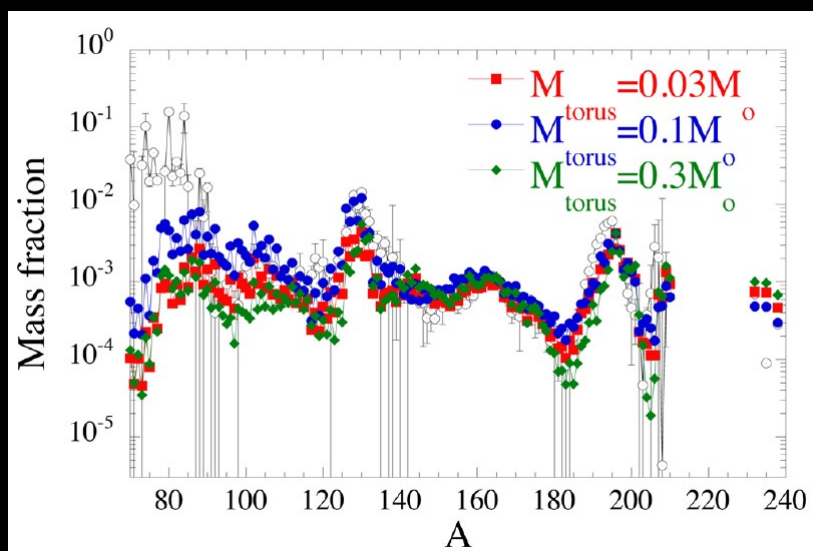
Metzger 2017

Interpretation - implications

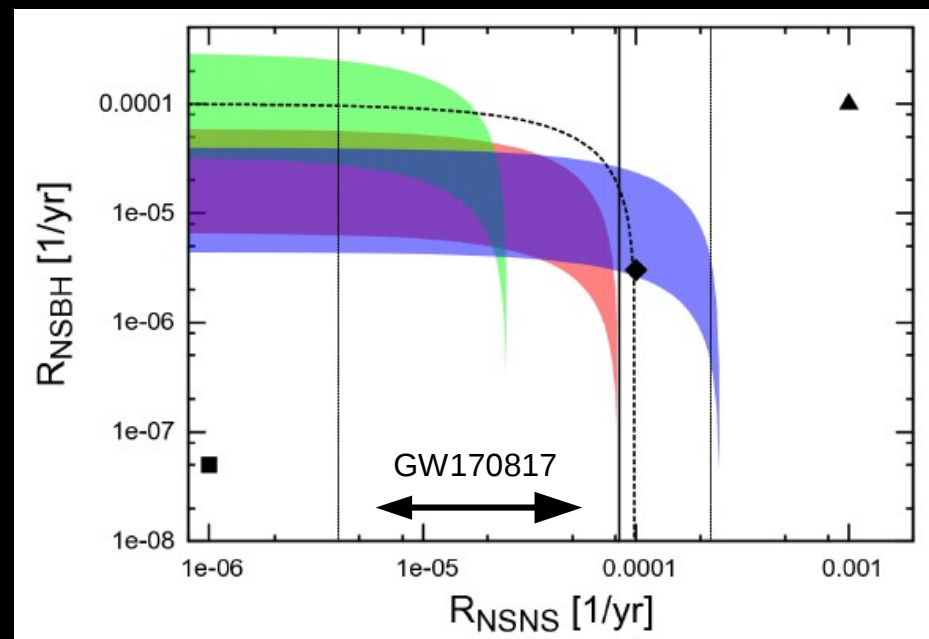
- ▶ heating and derived opacities are compatible with r-processing ejecta !!!
(not surprising for a theorist, see earlier work on r-process and em counterparts)
- ▶ Ejecta velocities and masses in ballpark of simulation results
- ▶ Derived ejecta masses are compatible with mergers being the main source of heavy r-process elements in the Universe

→ overall strong evidence that NS mergers play a prominent role for heavy element formation

Only $A > 130$



Just et al. 2015

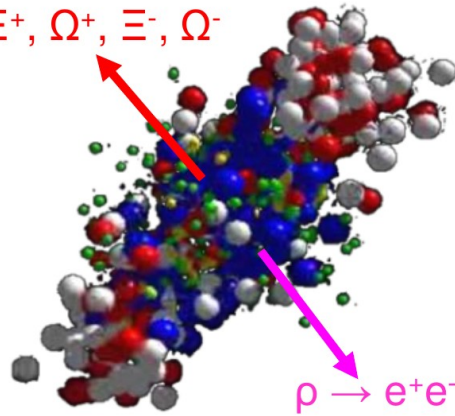


Bauswein et al. 2014

The high-density equation of state

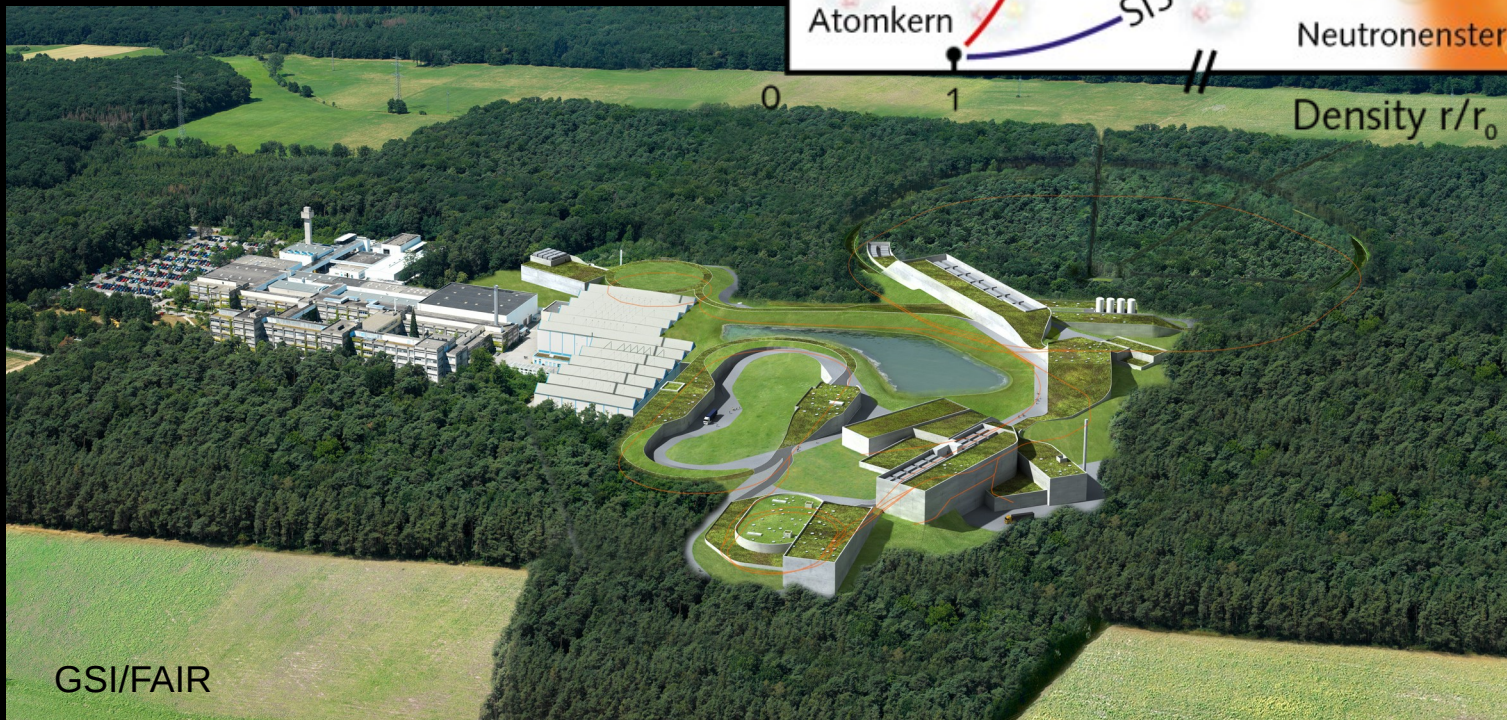
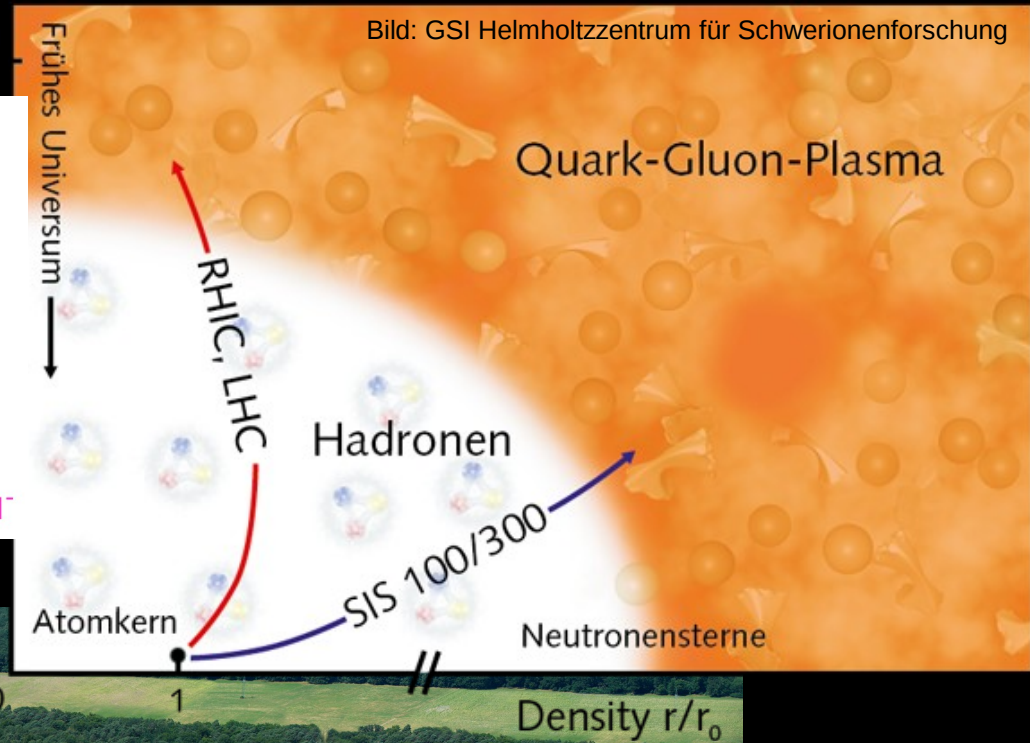
CBM collaboration

$\bar{p}, \bar{\Lambda}, \Xi^+, \Omega^+, \Xi^-, \Omega^-$

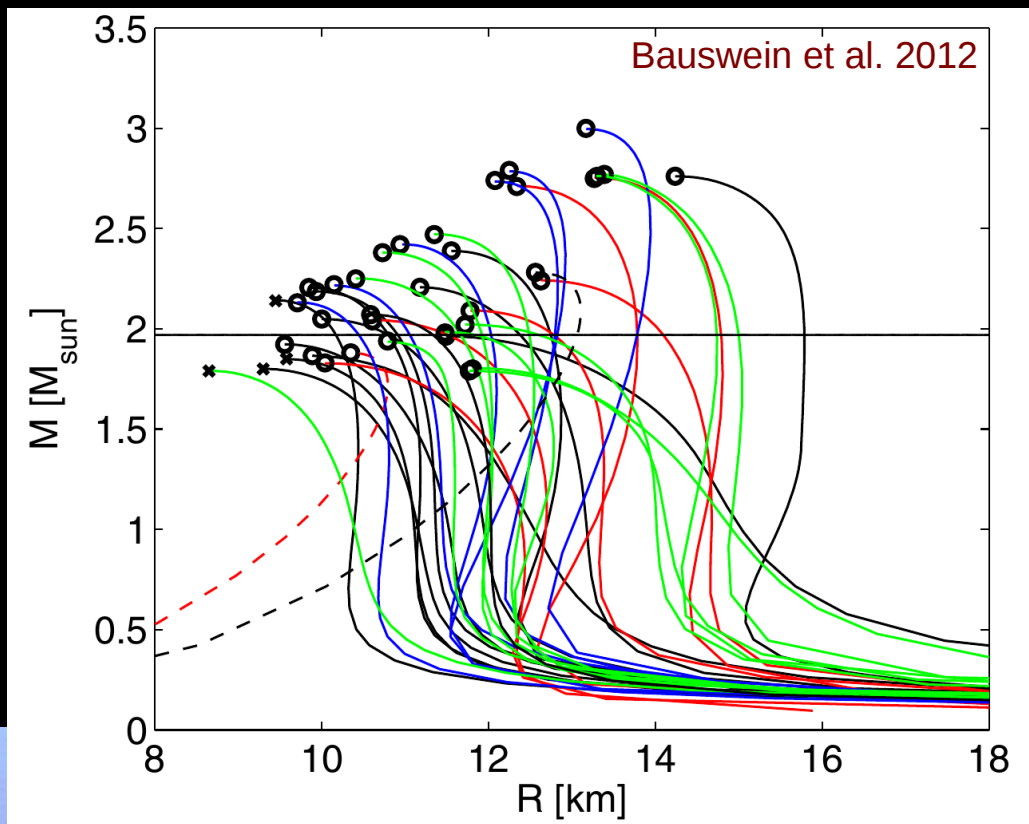
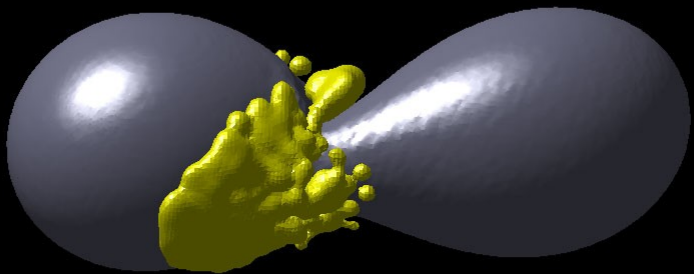


$\rho \rightarrow e^+e^-, \mu^+\mu^-$

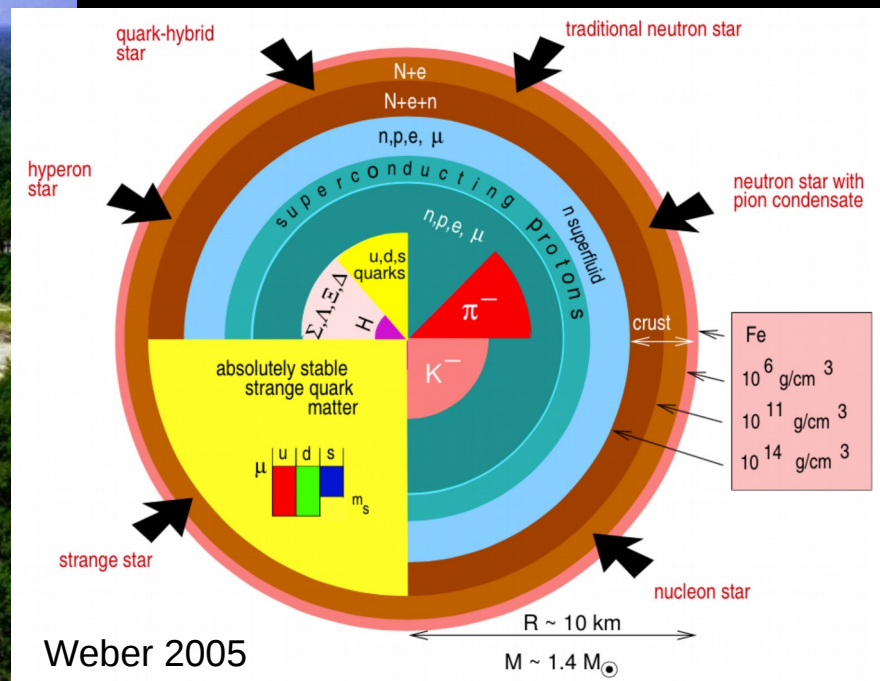
Figure 2: Snapshot of a collision between two gold nuclei at a beam energy of 10 GeV/nucleon according to a simulation. Particular interesting probes of the fireball matter are heavy anti-particles, particles which contain two or three strange quarks, and short-lived particles which decay inside the fireball into pairs of electrons or muons.



GSI/FAIR



Advanced LIGO



Relativistic hydrostatic equilibrium

- ▶ Tolman-Oppenheimer-Volkoff equations → enclosed mass $m(r)$ and pressure $P(r)$

$$\frac{dm(r)}{dr} = 4\pi r^2 \rho(P)$$

$$\frac{dP(r)}{dr} = -\frac{\rho(P)m}{r^2} \left(1 + \frac{P}{\rho(P)}\right) \left(1 + \frac{4\pi P r^3}{m}\right) \left(1 - \frac{2m}{r}\right)^{-1} \quad G = c = 1$$

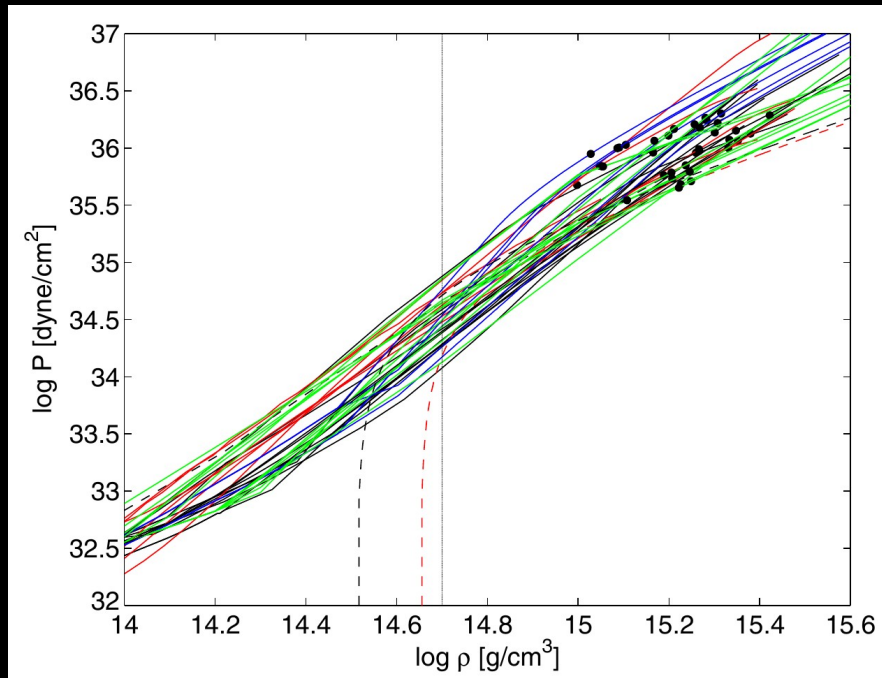
- ▶ System closed by EoS $P(\rho)$

→ stellar profiles, Mass-Radius relation (for given EoS)

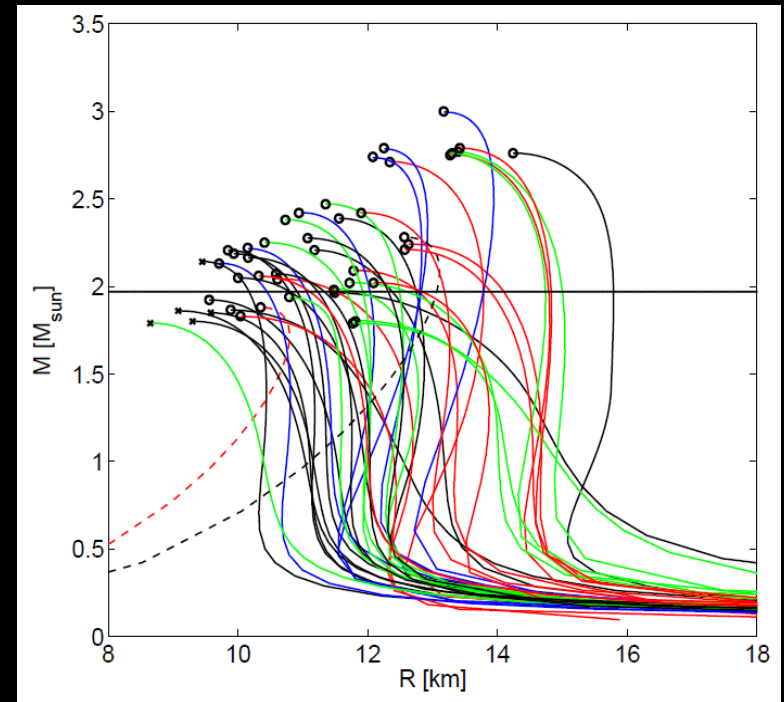
→ unique link between EoS and M-R relation

Unknown properties of EoS of NS matter

- ▶ Mass-radius relation (of non-rotating NSs) and EoS are uniquely linked through Tolman-Oppenheimer-Volkoff (TOV) equations



TOV



Theory: $P(\rho)$ \longleftrightarrow currently
future \longleftrightarrow Observation: $R(M)$

→ NS properties (of non-rotating stars) and EoS properties are equivalent !!!

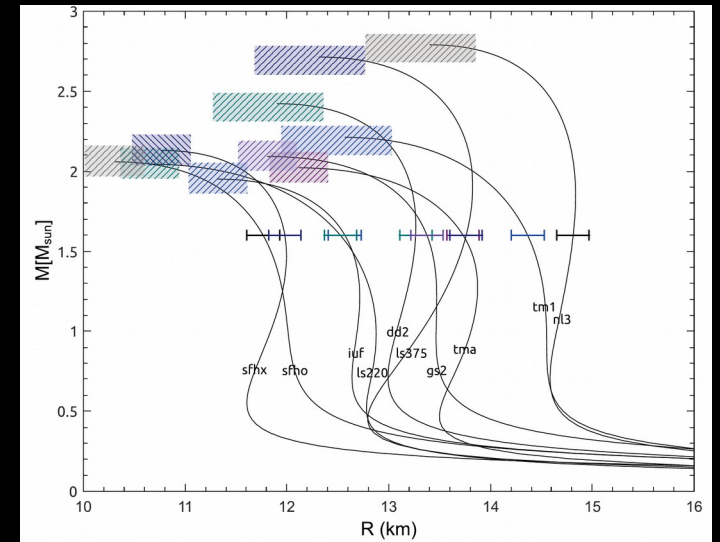
(not all displayed EoS compatible with all nuclear physics constraints)

EoS constraints

- ▶ Astrophysics perspective:

→ measure/constrain NS radii $R_{1.35}$, $R_{1.6}$, R_{\max}

→ measure/constrain M_{\max}

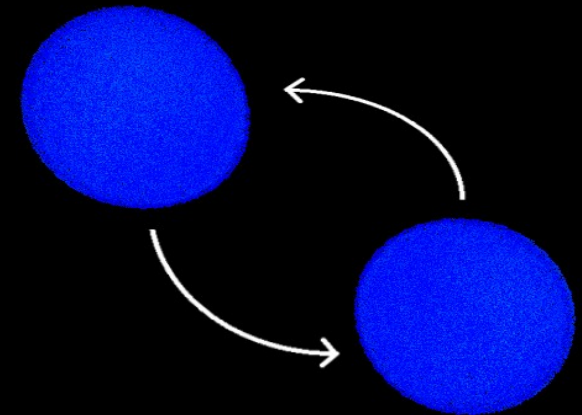


- ▶ many ideas around – GWs particularly appealing because systematics better under control
- ▶ (background: GWs are generated by 2nd time derivative of mass quadrupole)

$$h_{ij}^{TT} = \frac{2G}{c^4 r} \ddot{Q}_{ij}^{TT}$$

- ▶ Strategy: EoS and $R(M)$ fully equivalent

→ use TOV properties to characterize EoS impact



EoS constraints

(current and future approaches)

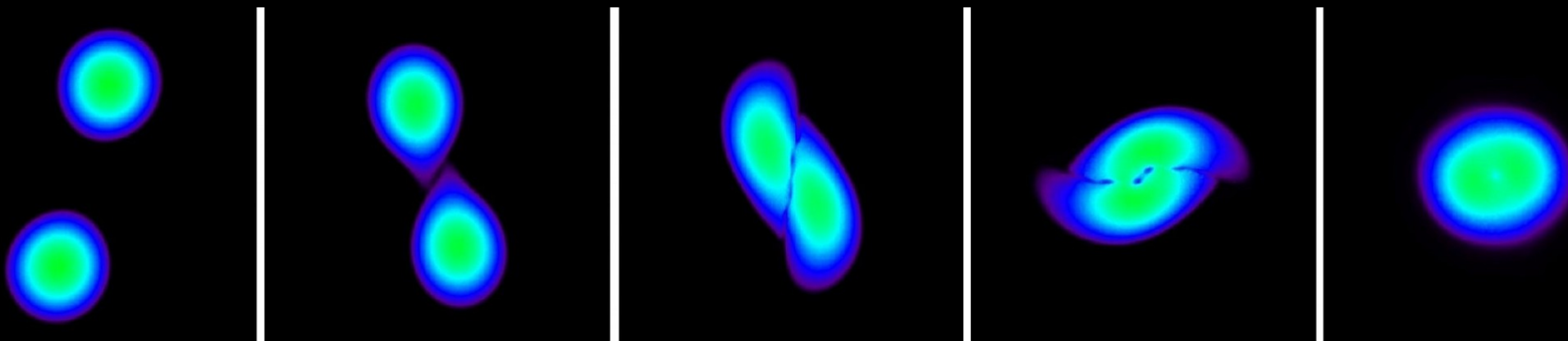
Goal: EoS from GWs

Three complementary strategies:

- ▶ Tidal effects during the inspiral → accelerate inspiral compared to BH-BH
- ▶ Oscillations of the postmerger remnant
- ▶ Collapse behavior

(keep in mind binary masses are relatively easy to measure, i.e. at low SNR !!!)

Finite-size effects during late inspiral



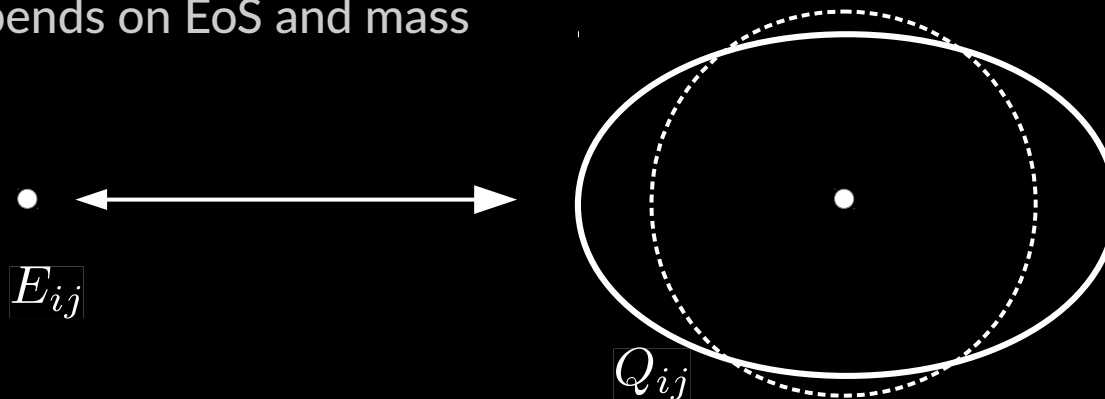
Description of tidal effects during inspiral

- ▶ Tidal field E_{ij} of one star induces change of quadrupole moment Q_{ij} of other component
- ▶ Changed quadrupole moment affects GW signal, especially phase evolution
→ inspiral faster compared to point-particle inspiral
- ▶ Strength of induced quadrupole moment depends on NS structure / EoS:

$$Q_{ij} = -\lambda(M) E_{ij}$$

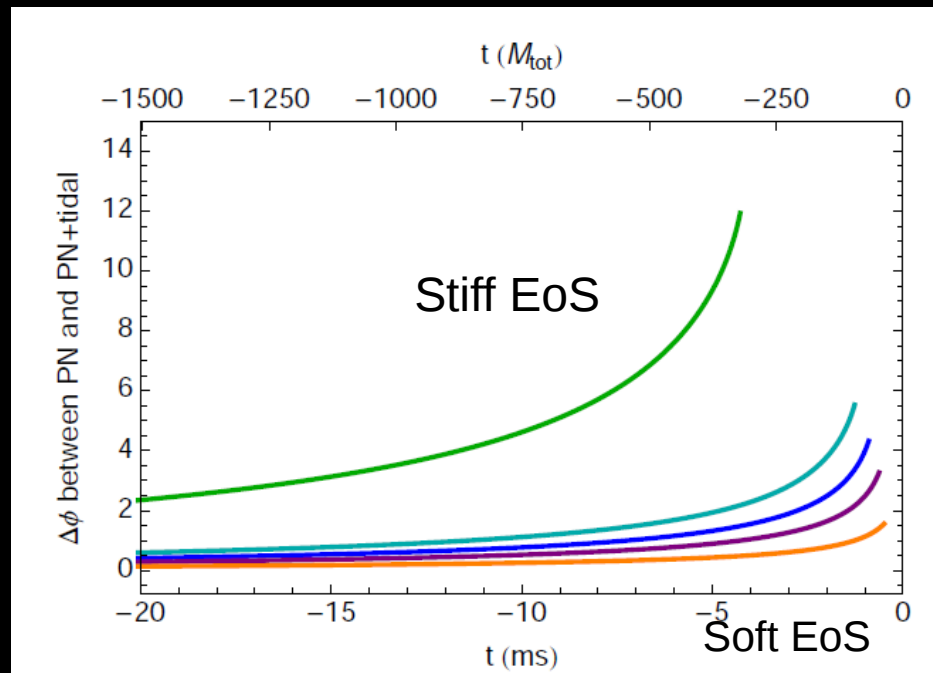
$$\lambda(M) = \frac{2}{3} k_2(M) R^5$$

- ▶ Tidal deformability depends on radius (clear – smaller stars are harder to deform) and “Love number” k_2 (~“TOV” properties)
- ▶ k_2 also depends on EoS and mass



Inspiral

- ▶ Orbital phase evolution affected by tidal deformability – only during last orbits before merging
- ▶ Inspiral accelerated compared to point-particle inspiral for larger Lambda
- ▶ Difference in phase between NS merger and point-particle inspiral:



e.g. Read et al. 2013

Merger time of point particle

EoS impact measured by tidal deformability

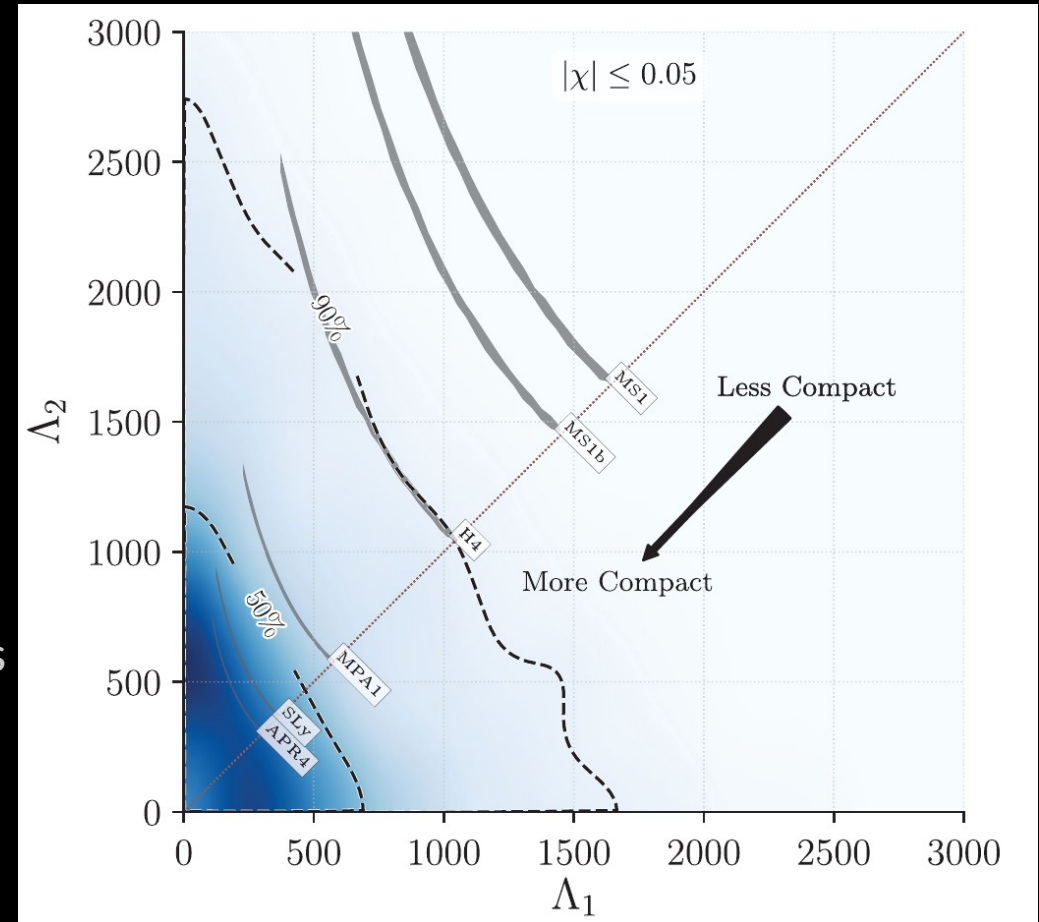
$$\Lambda(M) = \frac{2}{3} k_2(M) \left(\frac{c^2 R}{G M} \right)^5$$

Challenge: construct faithful templates for data analysis

Measurement

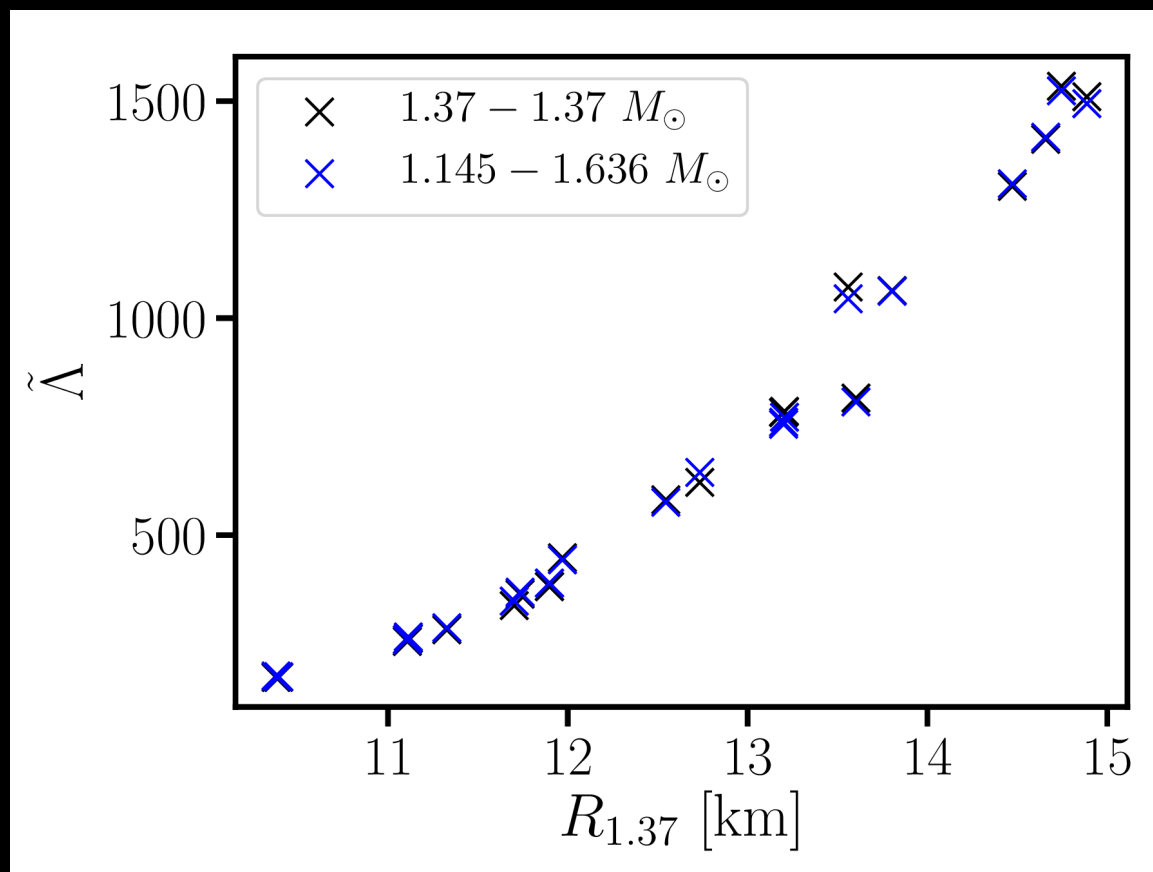
- ▶ $\Lambda < \sim 800$
→ Means that very stiff EoSs are excluded
- ▶ Recall uncertainties in mass measurements (only Mchirp accurate)
- ▶ systematic errors not included
→ ongoing research
- ▶ Better constraints expected in future as sensitivity increases

$$\tilde{\Lambda} = \frac{16(m_1 + 12m_2)m_1^4\Lambda_1 + (m_2 + 12m_1)m_2^4\Lambda_2}{13(m_1 + m_2)^5}$$



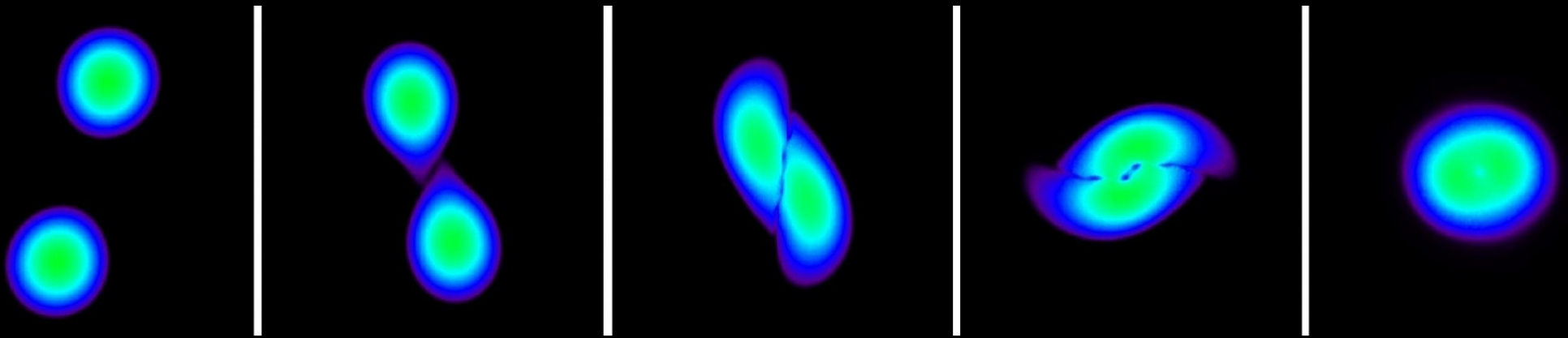
Abbott et al. 2017

► Tidal deformability vs. radius

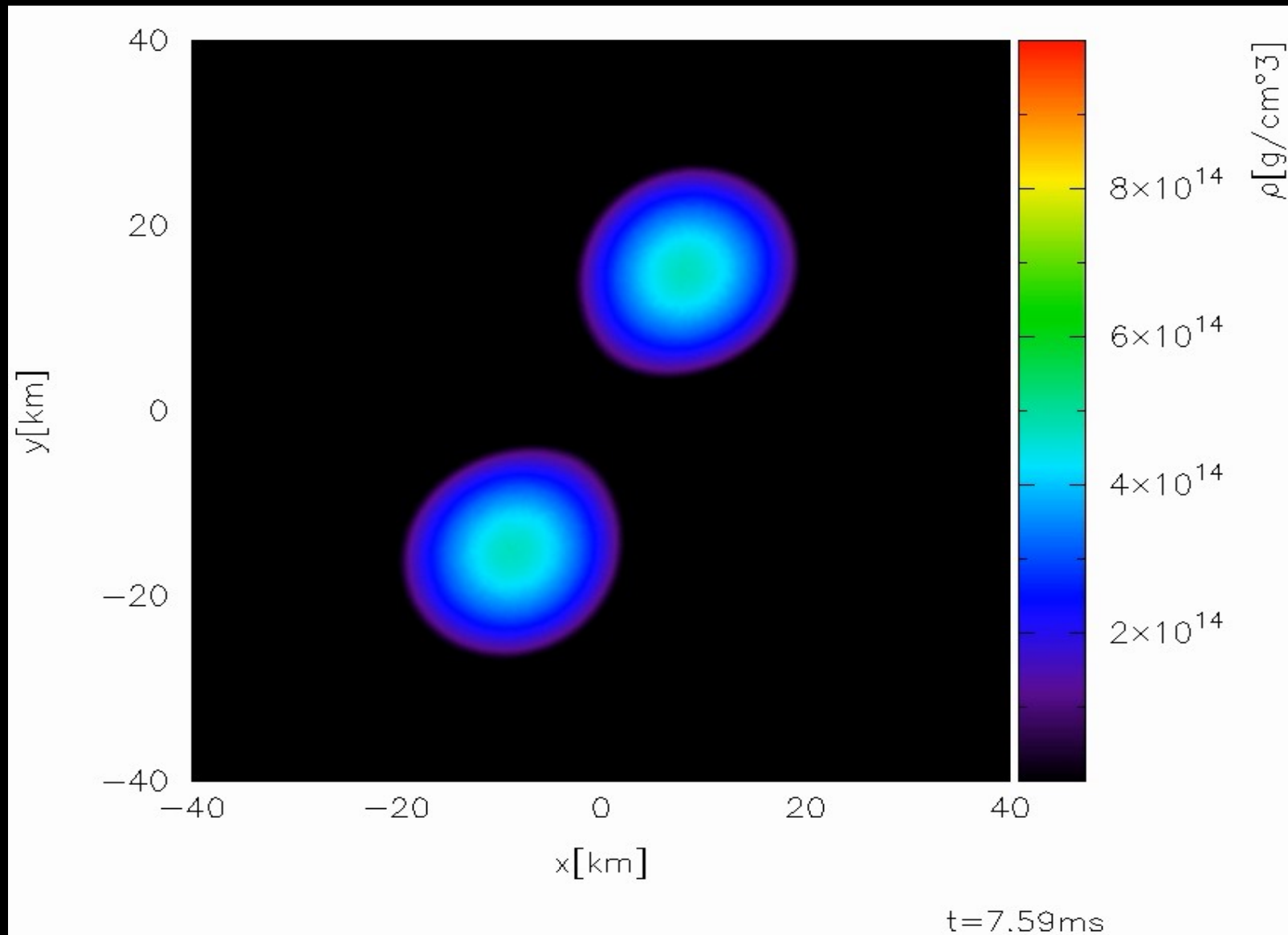


→ GW170817 constrains NS radii from above

Postmerger oscillations



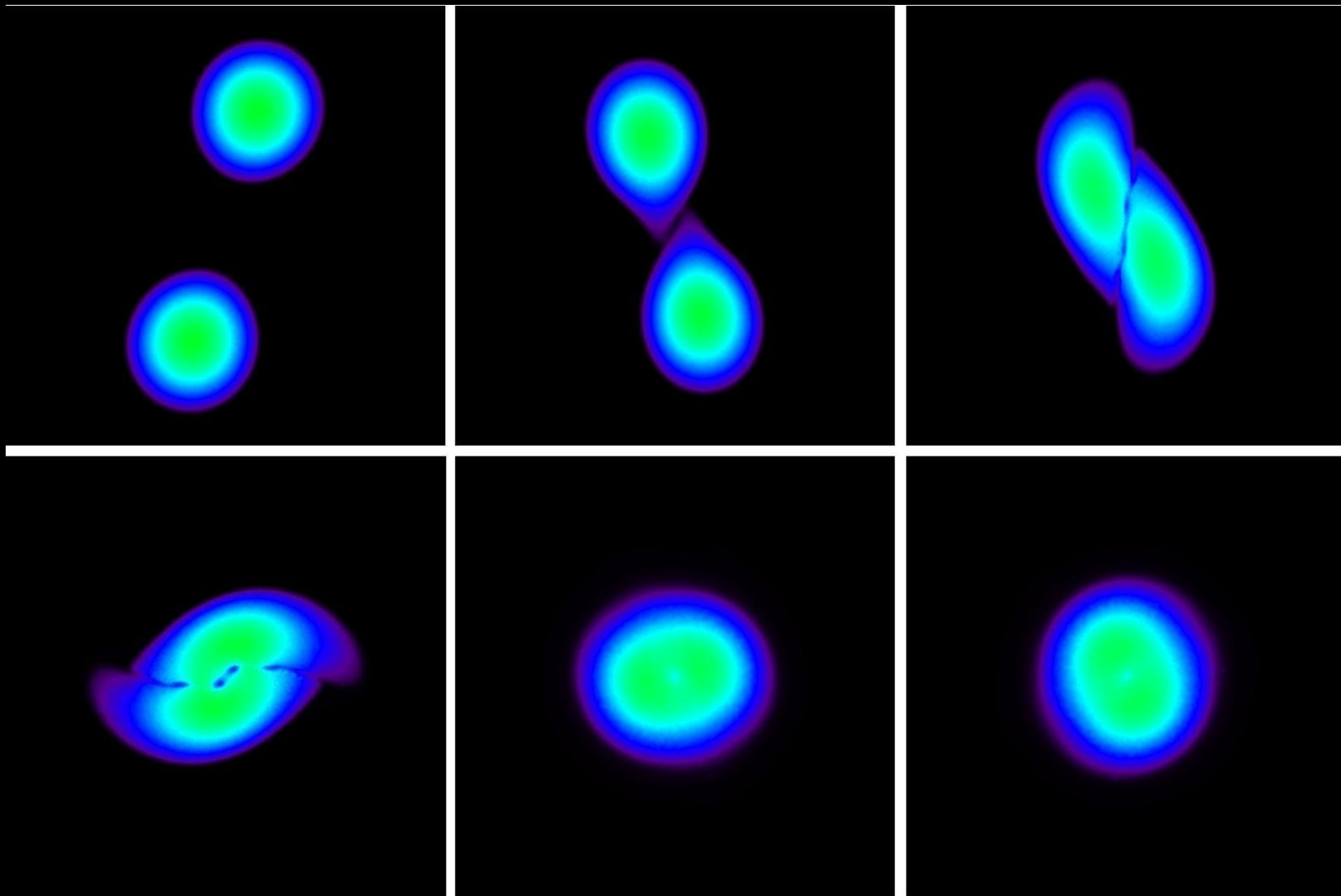
Simulation: $1.35+1.35 M_{\text{sun}}$



Density evolution in equatorial plane, Shen EoS

Relativistic smooth particle hydrodynamics, conformally flat spatial metric, microphysical temperature-dependent EoS

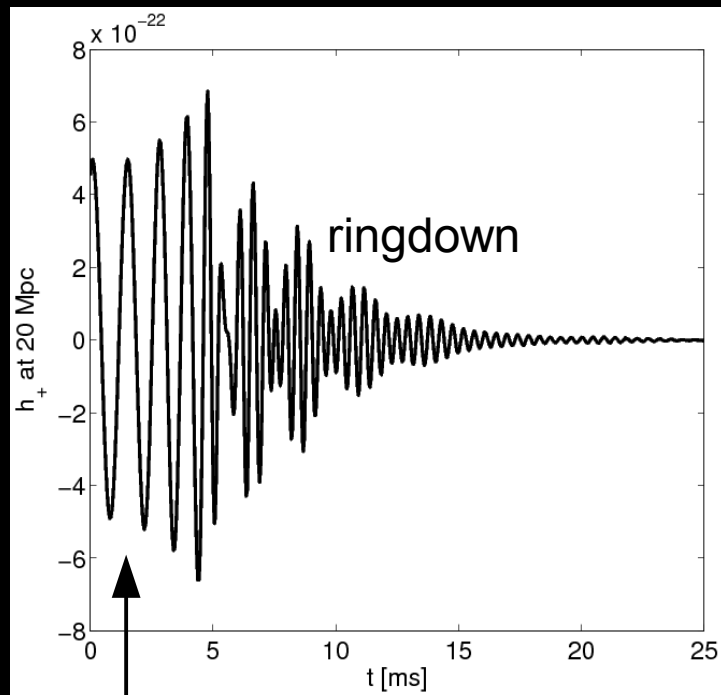
1.35-1.35 Msun, Shen EoS



Relativistic smooth particle hydrodynamics, conformally flat spatial metric,
microphysical temperature-dependent EoS

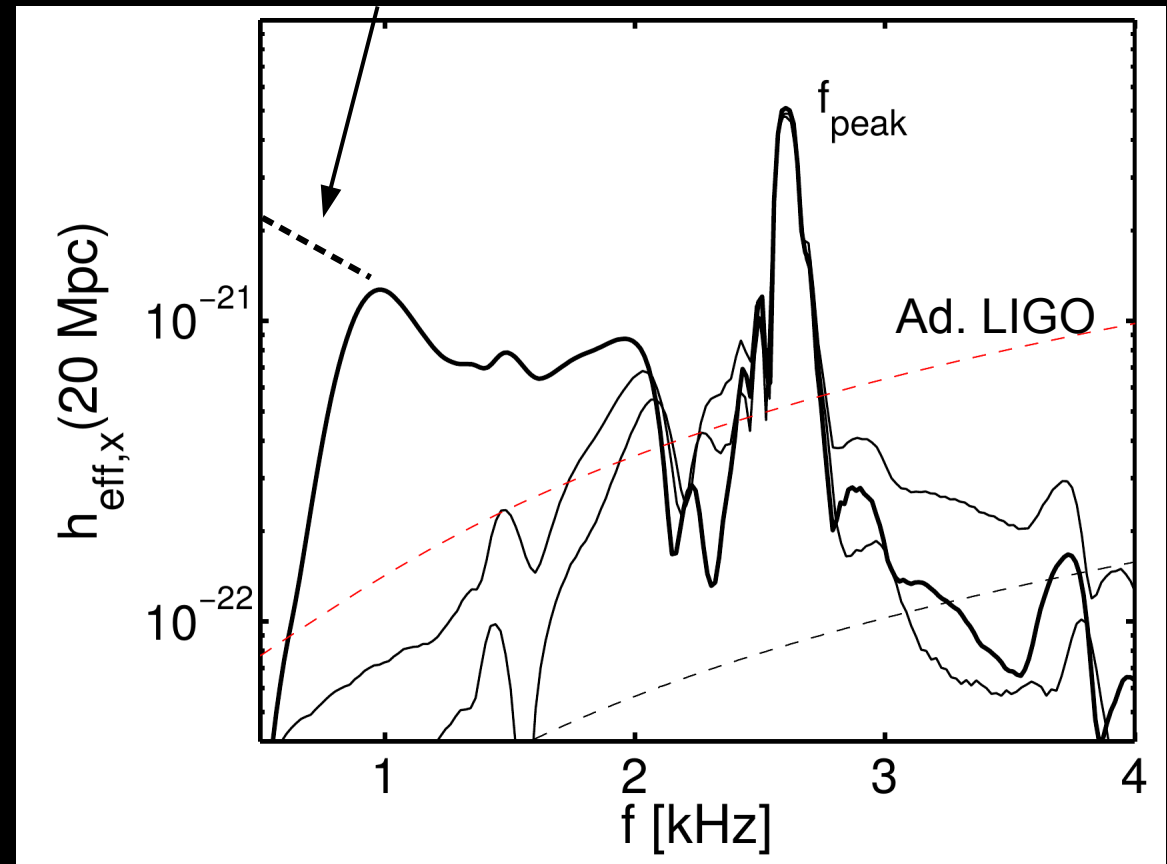
Postmerger

1.35-1.35 M_{sun} , 20 Mpc



Earlier inspiral

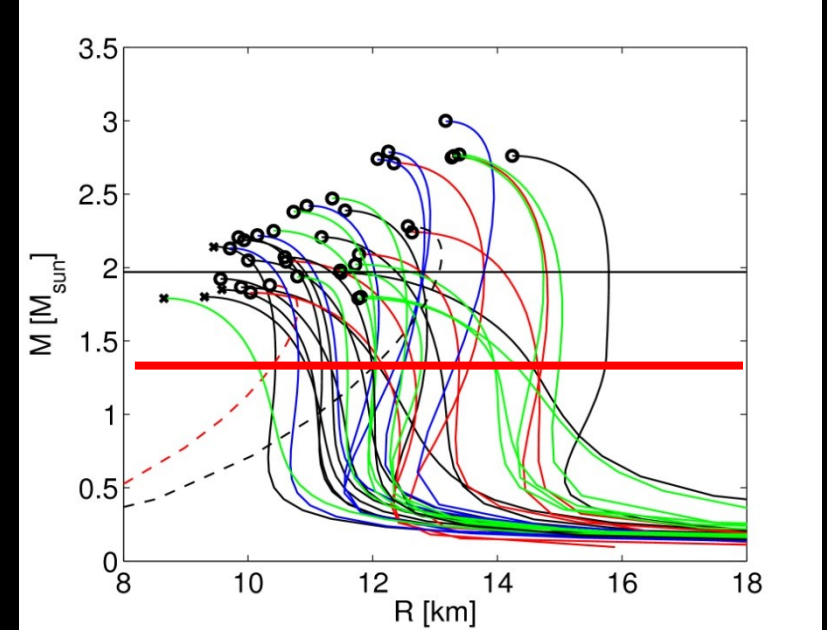
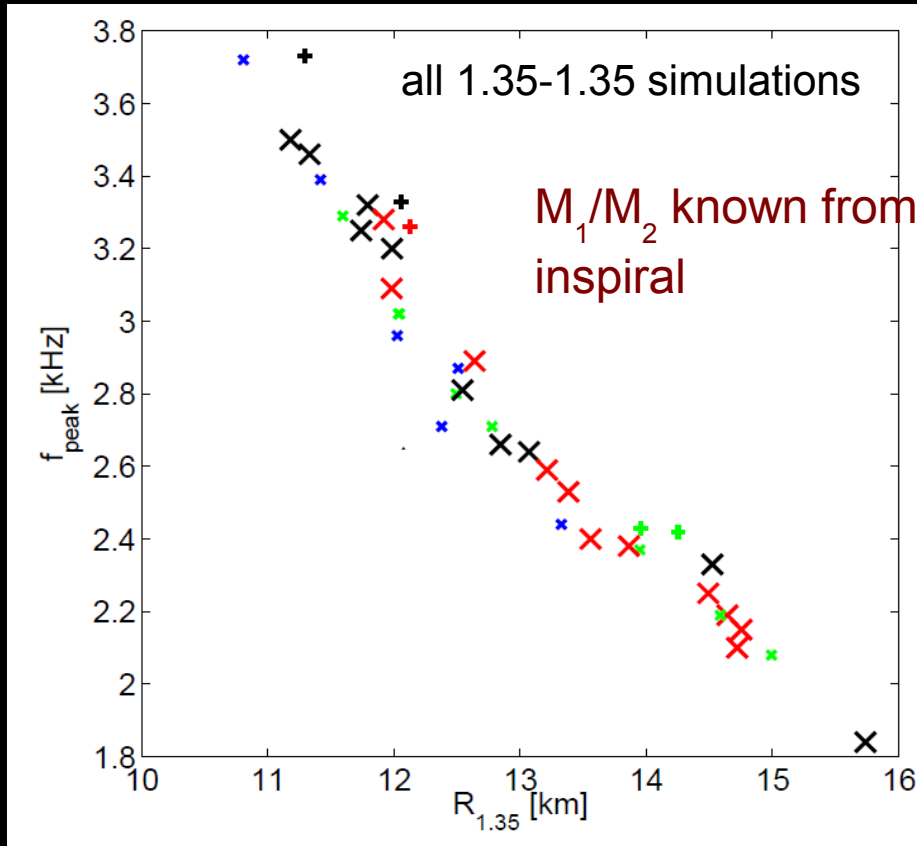
EoS



Dominant postmerger oscillation frequency f_{peak}

Very characteristic (robust feature in all models)

Every data point a single simulation of a $1.35\text{-}1.35 M_{\text{sun}}$ binary



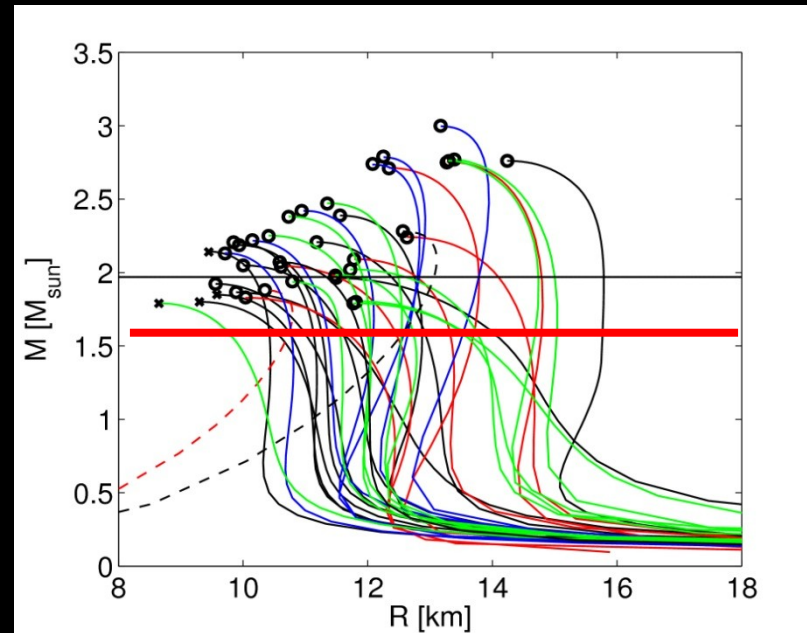
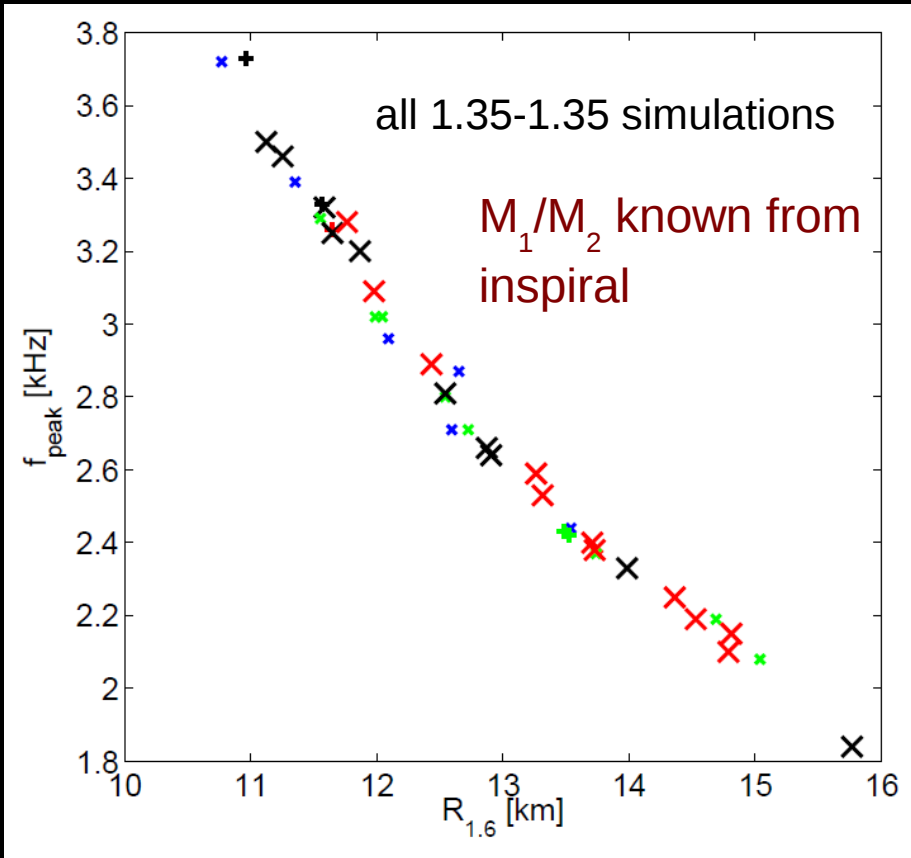
characterize EoS by radius of nonrotating NS with $1.35 M_{\text{sun}}$

Bauswein et al. 2012

Pure TOV property => **Radius measurement** via f_{peak}

→ **Empirical relation between GW frequency and NS radius (= our EoS parameter)**

Important: Simulations for the same binary mass, but with varied EoS
Recall that total mass can be measured quite accurately



characterize EoS by radius of nonrotating NS with $1.6 M_{\text{sun}}$

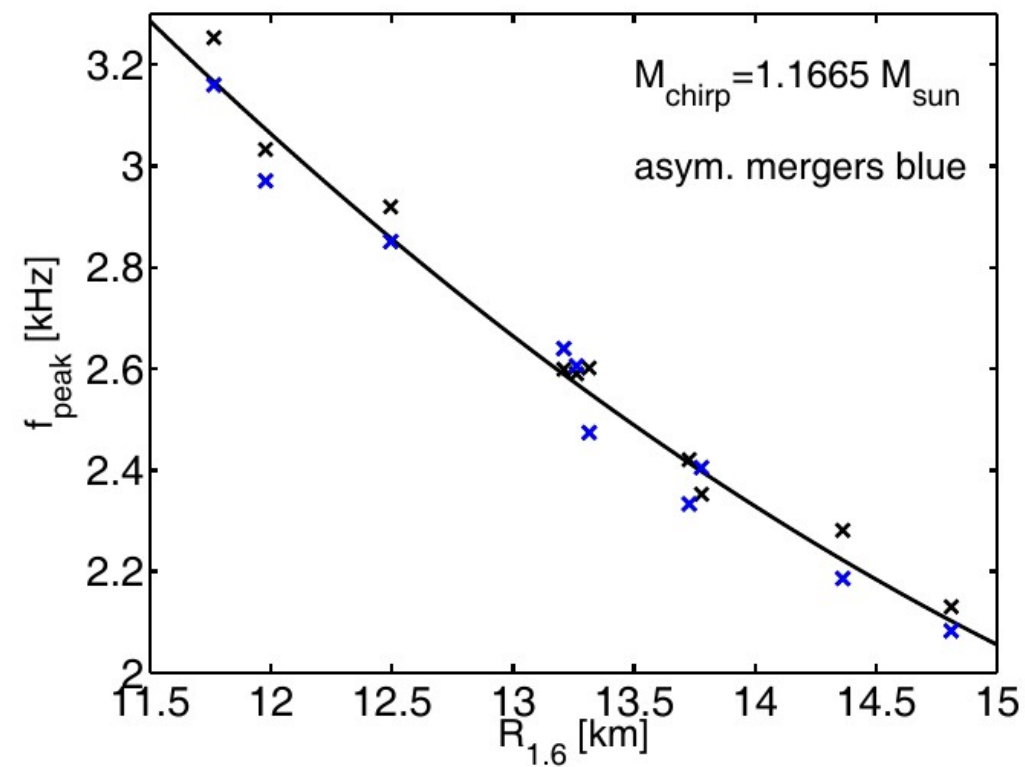
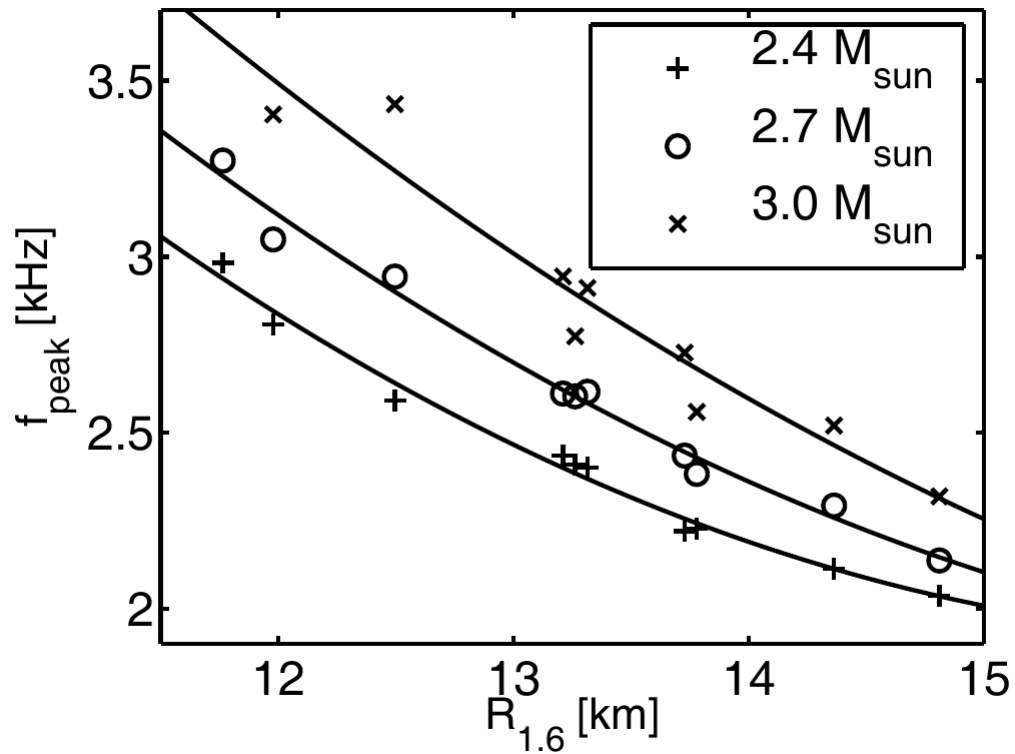
Bauswein et al. 2012

Pure TOV/EoS property => **Radius measurement** via f_{peak}

Fit: $R(1.6 M_{\odot}) = 1.1 f_{GW}^2 - 8.6 f_{GW} + 28.$

Important: Simulations for the same binary mass, just with varied EoS

Binary mass variations



Different total binary masses
(symmetric)

Fixed chirp mass (asymmetric 1.2-1.5
 M_{sun} binaries and symmetric 1.34-
1.34 M_{sun} binaries)

GW data analysis

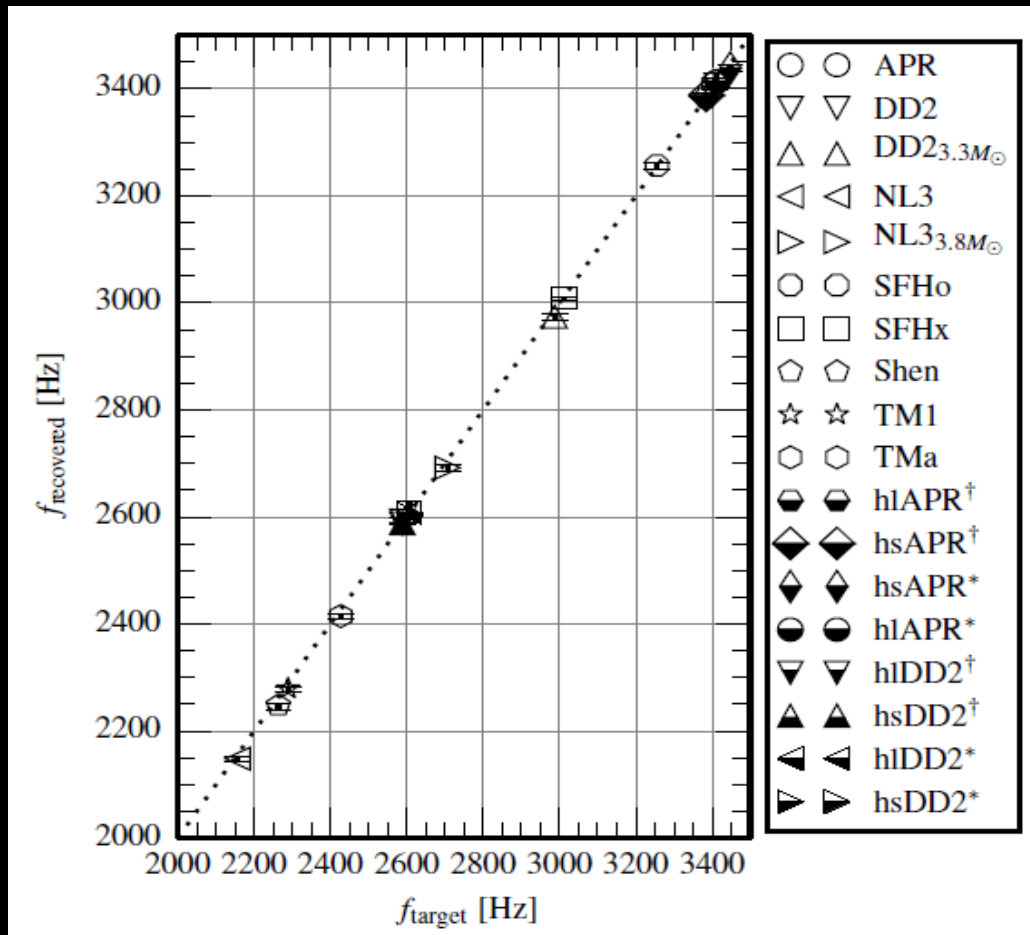
Searches performed for GW170817, but only upper limits - not surprising

→ but very promising at design sensitivity

→ data analysis - ongoing research

Data analysis – prove of principle

► Unmodeled burst search



Model waveforms hidden in rescaled LIGO noise

Peak frequency recovered with burst search analysis

Error ~ 10 Hz

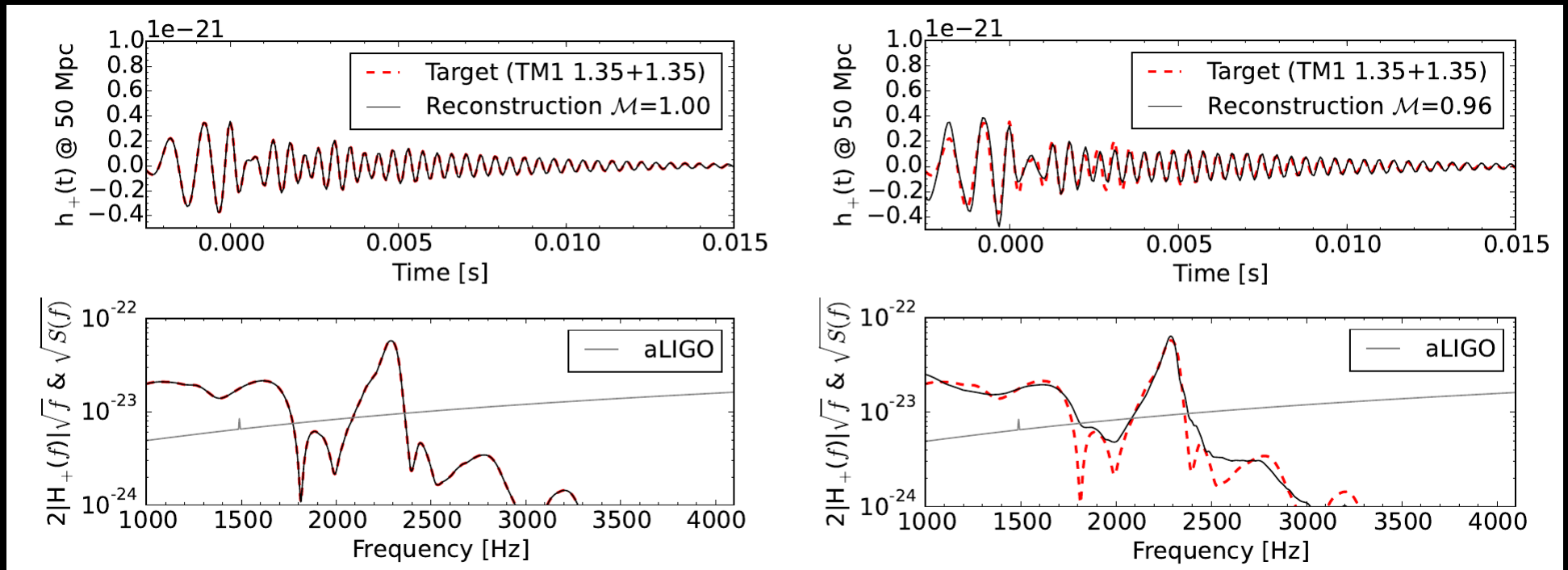
For signals within ~10-25 Mpc

=> for near-by event radius measurable with high precision (~0.01-1/yr)

Proof-of-principle study
→ improvements likely

Data analysis

► Principal Component analysis



Excluding recovered waveform from catalogue

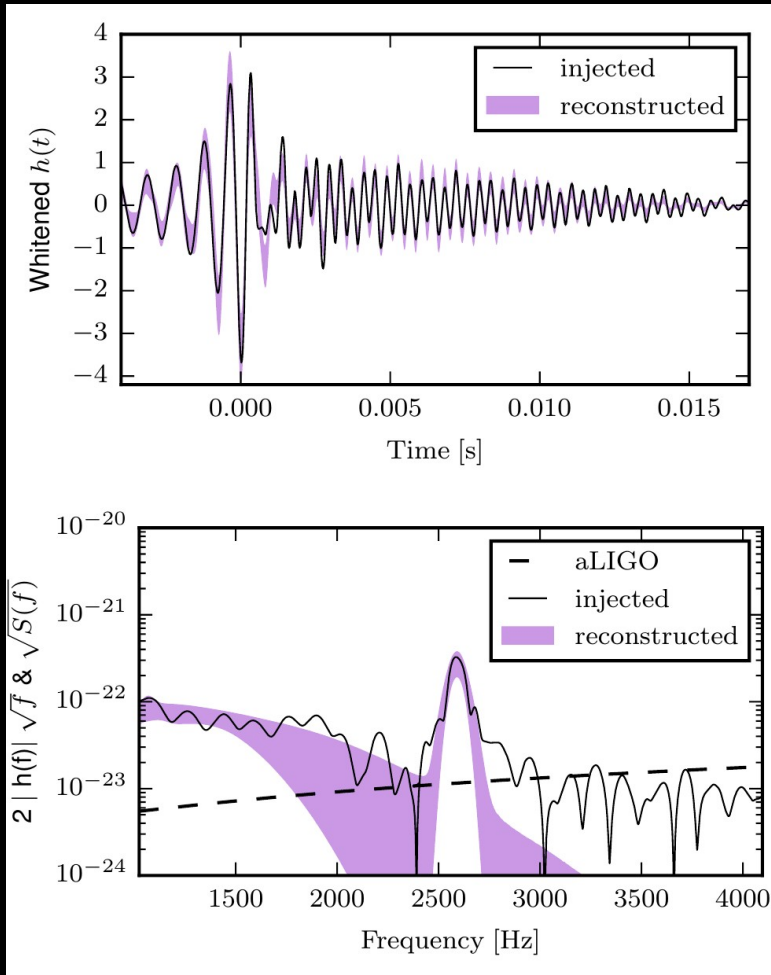
Clark et al. 2016

| Instrument | SNR_{full} | D_{hor} [Mpc] | \dot{N}_{det} [year^{-1}] |
|------------|-----------------------------------------|--------------------------------------------|-----------------------------------------------|
| aLIGO | 2.99 ^{3.86} _{2.37} | 29.89 ^{38.57} _{23.76} | 0.01 ^{0.03} _{0.01} |
| A+ | 7.89 ^{10.16} _{6.25} | 78.89 ^{101.67} _{62.52} | 0.13 ^{0.20} _{0.10} |
| LV | 14.06 ^{18.13} _{11.16} | 140.56 ^{181.29} _{111.60} | 0.41 ^{0.88} _{0.21} |
| ET-D | 26.65 ^{34.28} _{20.81} | 266.52 ^{342.80} _{208.06} | 2.81 ^{5.98} _{1.33} |
| CE | 41.50 ^{53.52} _{32.99} | 414.62 ^{535.22} _{329.88} | 10.59 ^{22.78} _{5.33} |

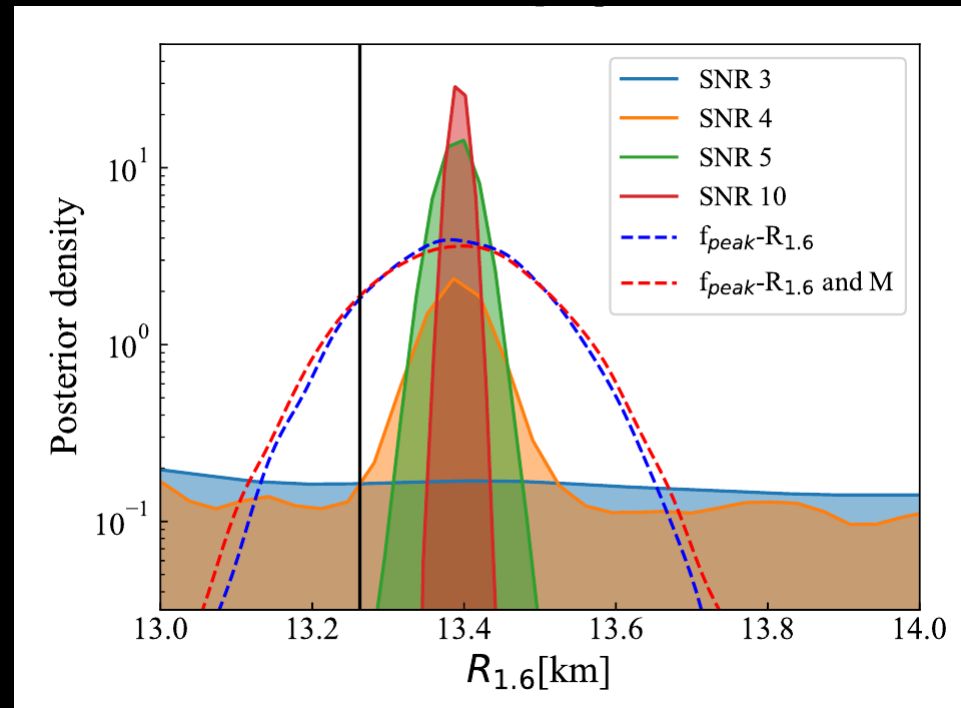
Outdated!!!

→ possible at Ad. LIGO's design sensitivity!

Model-agnostic data analysis



Based on wavelets

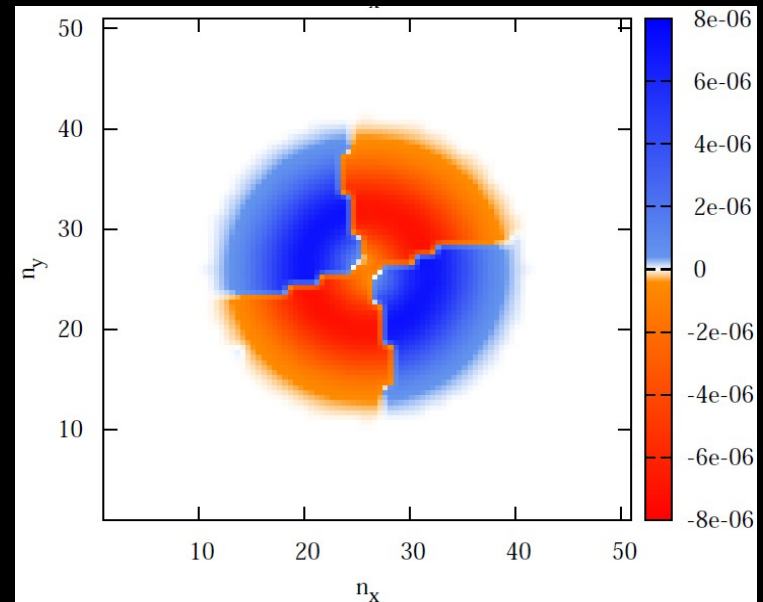
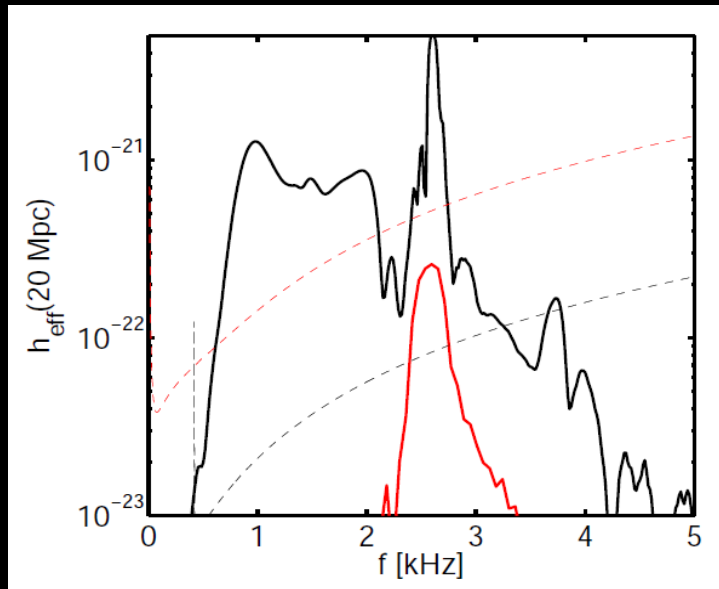


Chatziioannou et al. (2017)

Future

Background

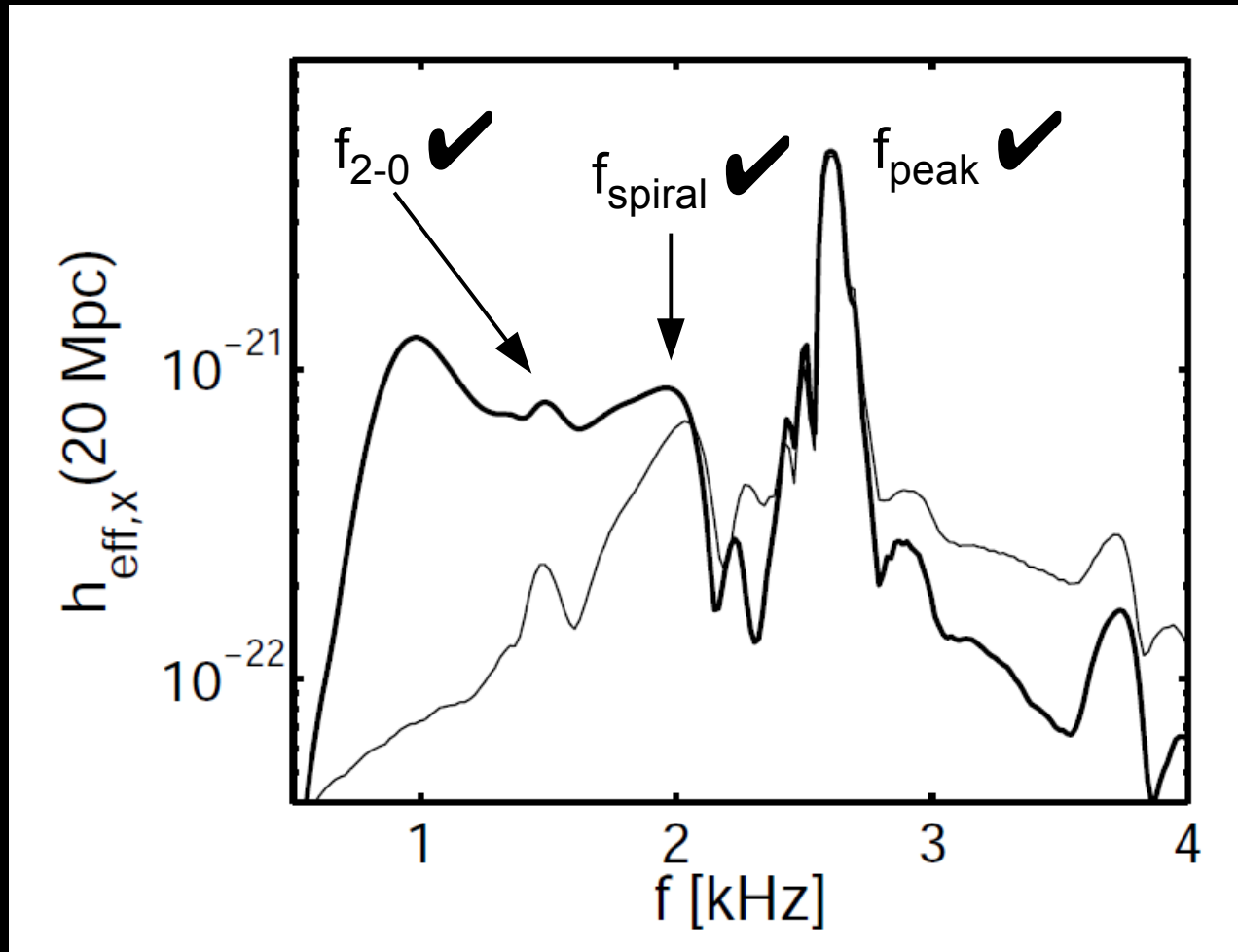
- ▶ Merger remnant is massive rotating star: many oscillation modes excited
- ▶ Only some modes / GW emission mechanisms identified
 - GW spectrum full of information
 - future: establish asteroseismology of merger remnants
 - probe inner structure of NSs – details of the EoS



Re-excitation of f-mode (Bauswein et al. 2016)

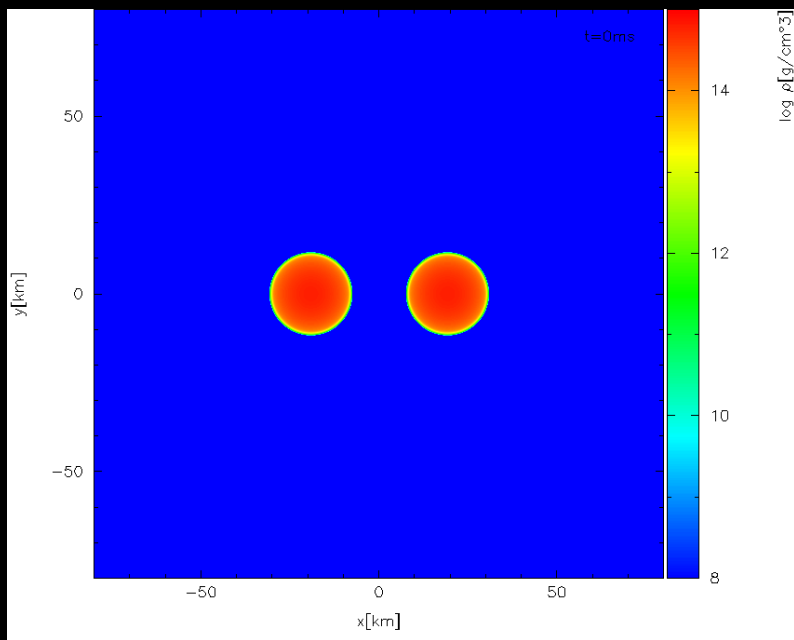
Eigen function (Stergioulas et al. 2011)

Typical GW spectrum



Identification and unified classification scheme of secondary GW features/modes
(Bauswein & Stergioulas 2015)

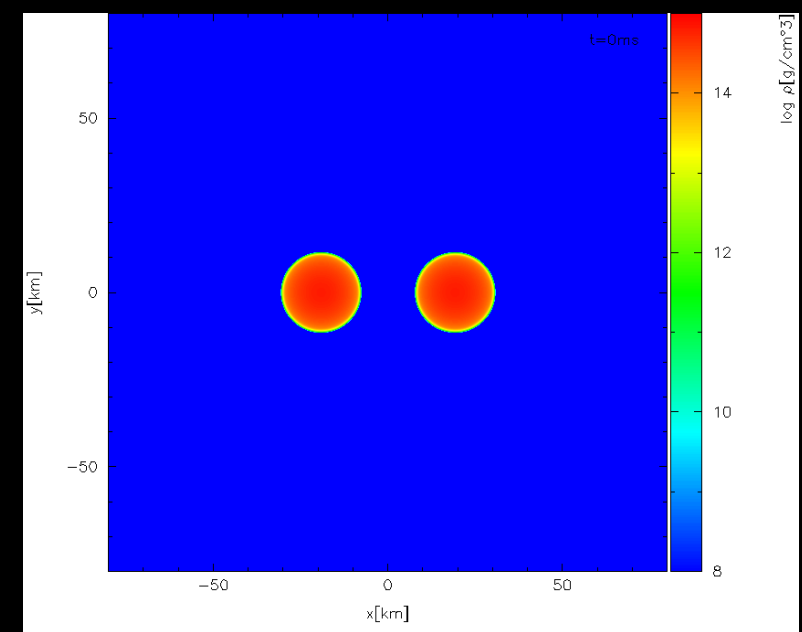
Collapse behavior



$$M_{\text{tot}} = 3.4 M_{\odot}$$



$$M_{\text{tot}} = 3.5 M_{\odot}$$



Shen EoS

Collapse behavior: Prompt vs. delayed (/no) BH formation

Relevant for:

EoS constraints through M_{max} measurement

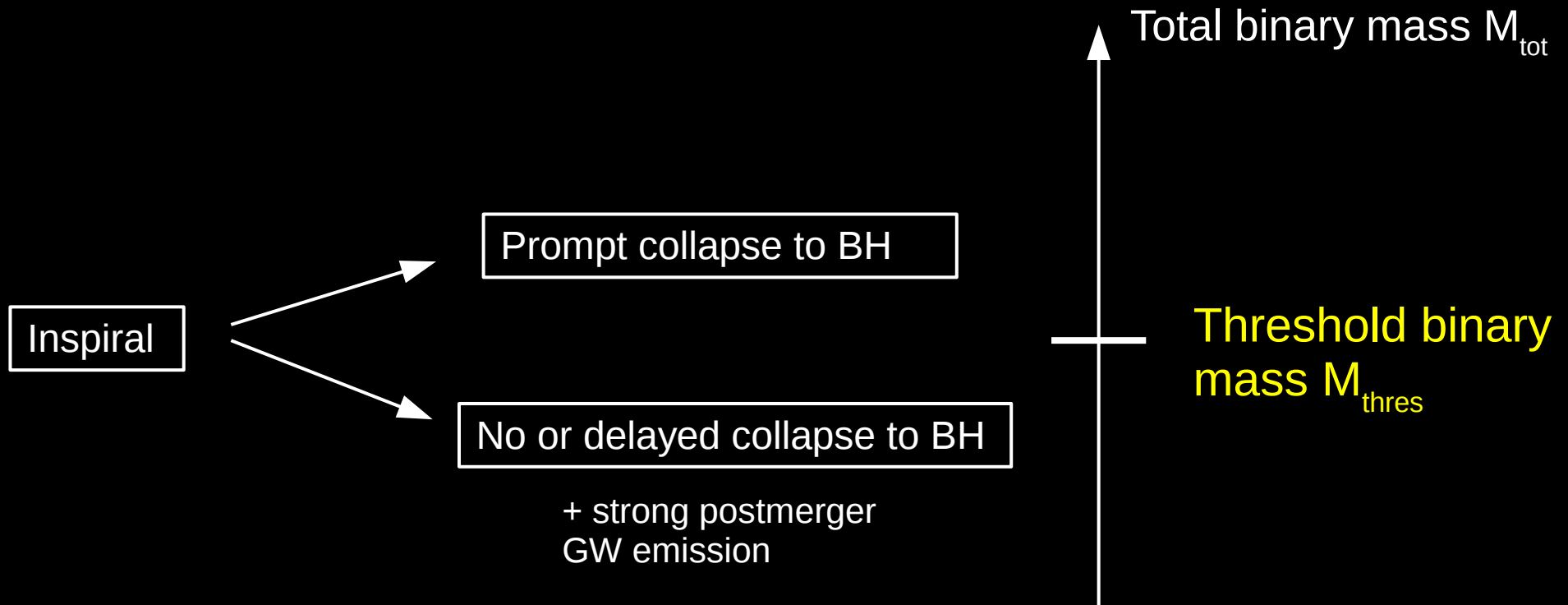
Conditions for short GRBs

Mass ejection

Electromagnetic counterparts powered by thermal emission

And NS radius constraints !!!

Collapse behavior



EoS dependent - somehow M_{max} should play a role

EoS constraints from GW170817

Simulations reveal M_{thres}

| EoS | M_{max} (M_{\odot}) | R_{max} (km) | C_{max} | $R_{1.6}$ (km) | M_{thres} (M_{\odot}) |
|-------------|-------------------------------------|--------------------------|------------------|-------------------|---------------------------------------|
| NL3 [37,38] | 2.79 | 13.43 | 0.307 | 14.81 | 3.85 |
| GS1 [39] | 2.75 | 13.27 | 0.306 | 14.79 | 3.85 |
| LS375 [40] | 2.71 | 12.34 | 0.325 | 13.71 | 3.65 |
| DD2 [38,41] | 2.42 | 11.90 | 0.300 | 13.26 | 3.35 |
| Shen [42] | 2.22 | 13.12 | 0.250 | 14.46 | 3.45 |
| TM1 [43,44] | 2.21 | 12.57 | 0.260 | 14.36 | 3.45 |
| SFHX [45] | 2.13 | 10.76 | 0.292 | 11.98 | 3.05 |
| GS2 [46] | 2.09 | 11.78 | 0.262 | 13.31 | 3.25 |
| SFHO [45] | 2.06 | 10.32 | 0.294 | 11.76 | 2.95 |
| LS220 [40] | 2.04 | 10.62 | 0.284 | 12.43 | 3.05 |
| TMA [44,47] | 2.02 | 12.09 | 0.247 | 13.73 | 3.25 |
| IUF [38,48] | 1.95 | 11.31 | 0.255 | 12.57 | 3.05 |

Bauswein et al. 2013

- ▶ ... meanwhile many more models

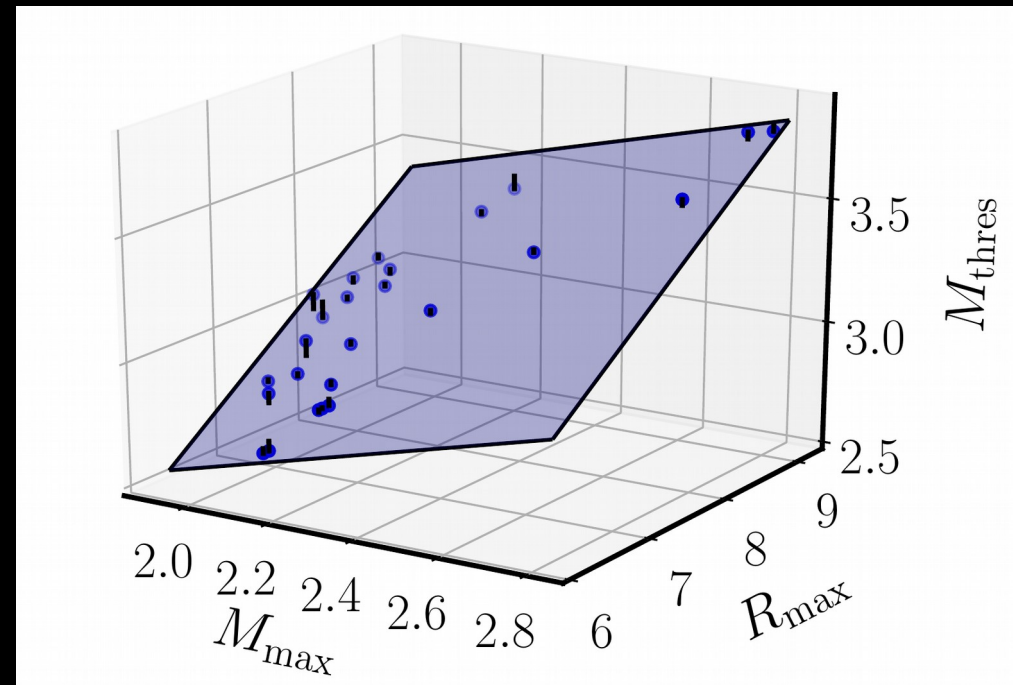
Threshold binary mass

- ▶ Empirical relation from simulations with different M_{tot} and EoS
- ▶ Fits (to good accuracy):

$$M_{\text{thres}} = M_{\text{thres}}(M_{\text{max}}, R_{1.6}) = \left(-3.6 \frac{G M_{\text{max}}}{c^2 R_{1.6}} + 2.38 \right) M_{\text{max}}$$

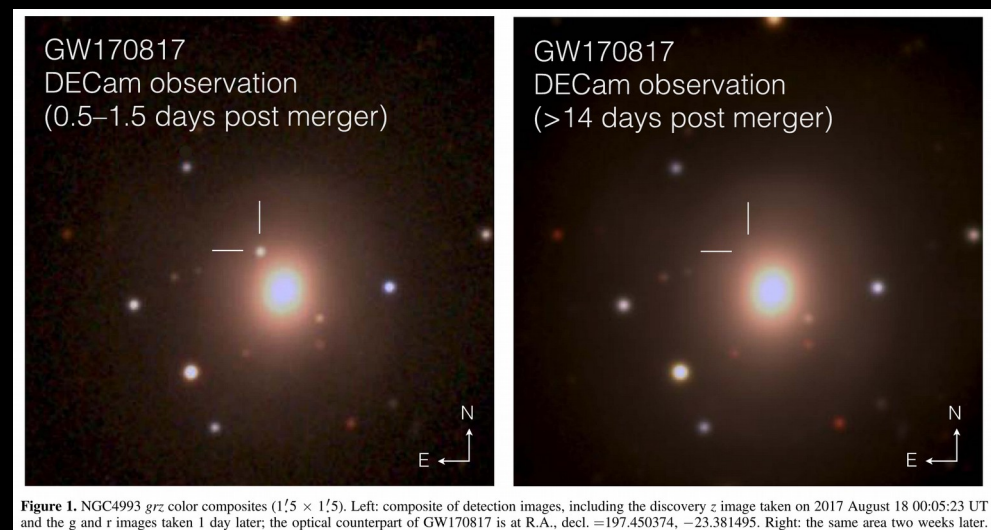
$$M_{\text{thres}} = M_{\text{thres}}(M_{\text{max}}, R_{\text{max}}) = \left(-3.38 \frac{G M_{\text{max}}}{c^2 R_{\text{max}}} + 2.43 \right) M_{\text{max}}$$

- ▶ Both better than $0.06 M_{\text{sun}}$



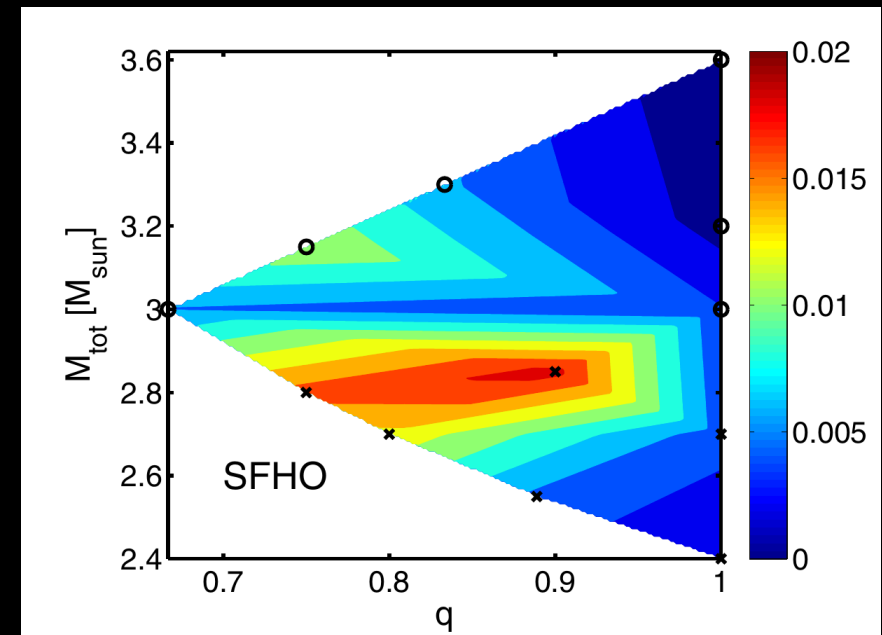
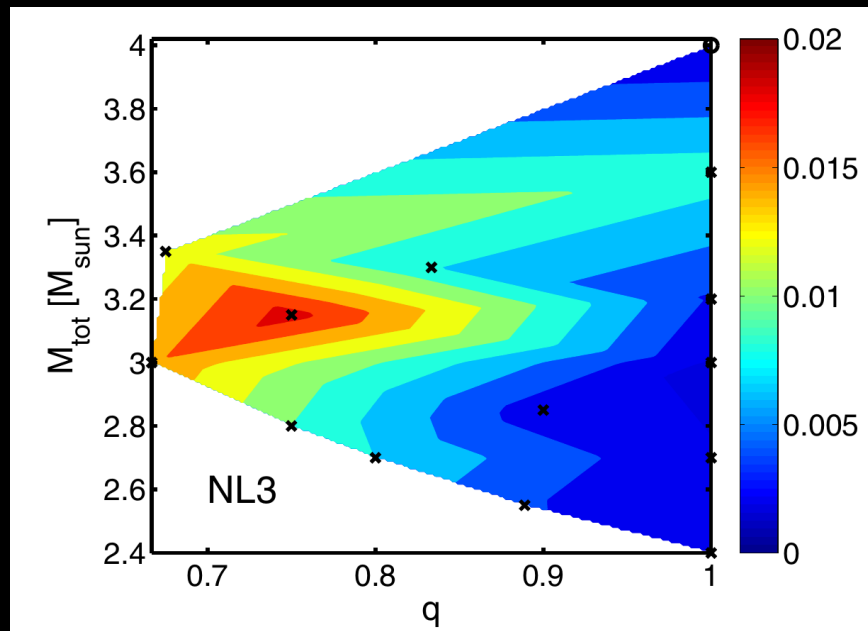
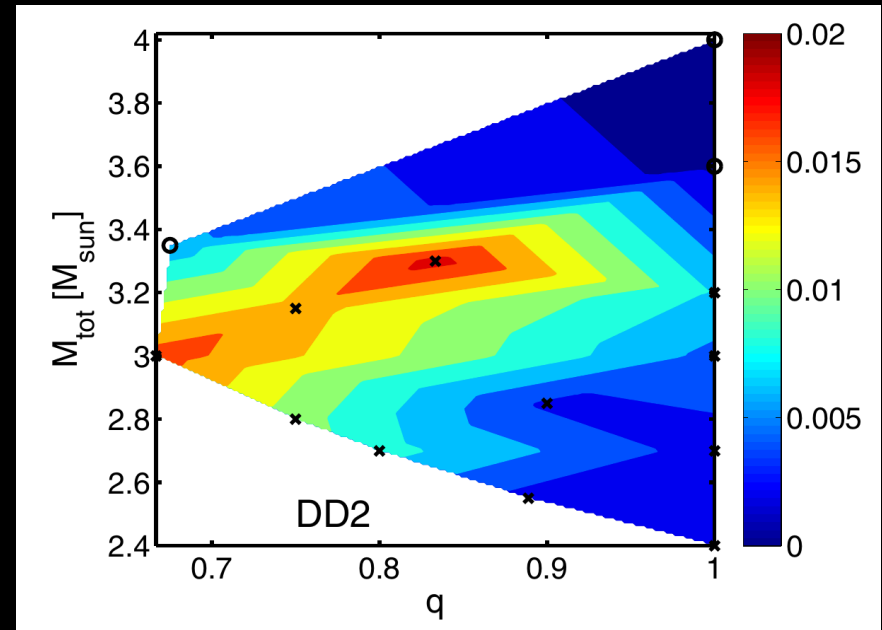
A simple but robust NS radius constraint from GW170817

- ▶ GW measurements reveal binary masses of merger very accurately:
 - total binary mass quite well: $2.74 M_{\text{sun}}$ for GW170817
 - mass ratio harder to measure: 0.7-1.0 for GW170817
- ▶ High ejecta mass inferred from optical transient
 - provides strong support for a delayed/no collapse in GW170817
 - even asymmetric mergers that directly collapse do not produce such massive ejecta

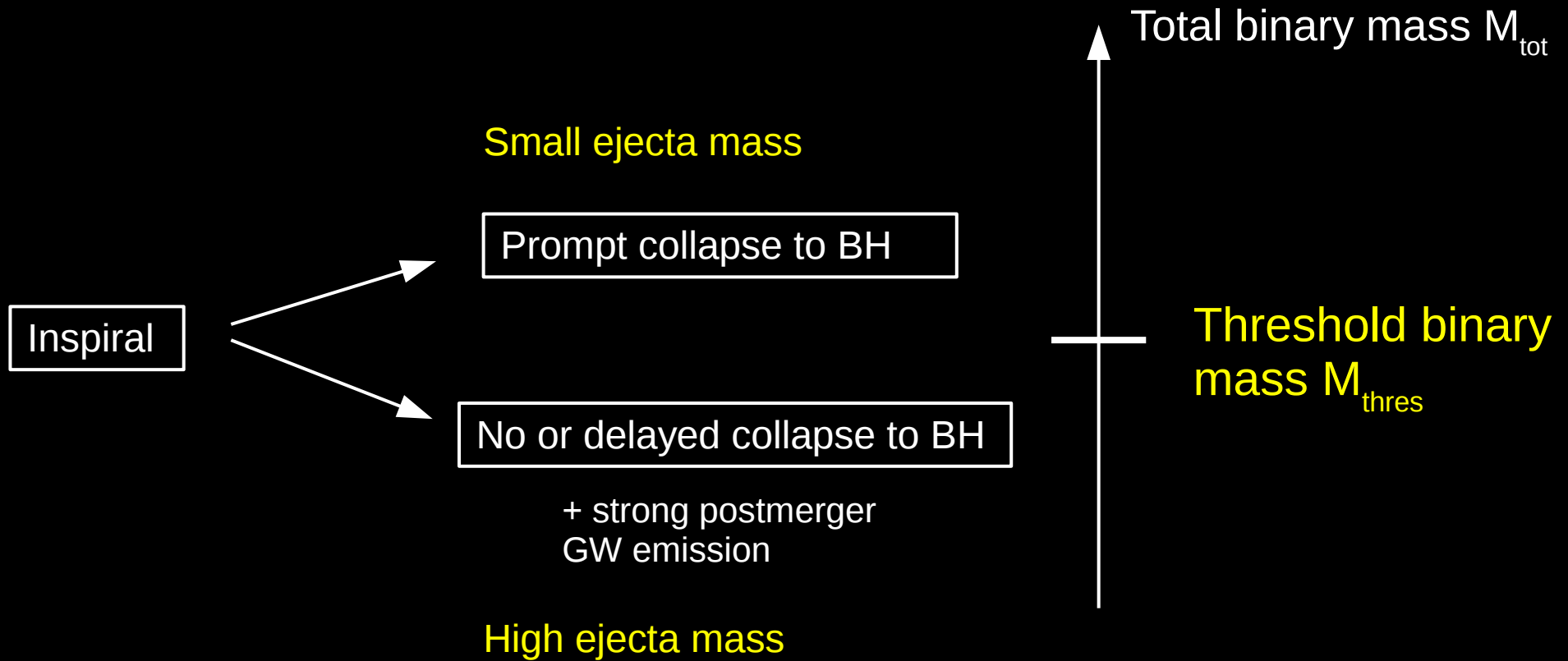


- ▶ Ejecta masses depend on EoS and binary masses
- ▶ Note: high mass points already to soft EoS (tentatively/qualitatively)
- ▶ Prompt collapse leads to reduced ejecta mass
- ▶ Light curve depends on ejecta mass:
→ 0.02 - 0.05 Msun point to delayed collapse
- ▶ Note: here only dynamical ejecta

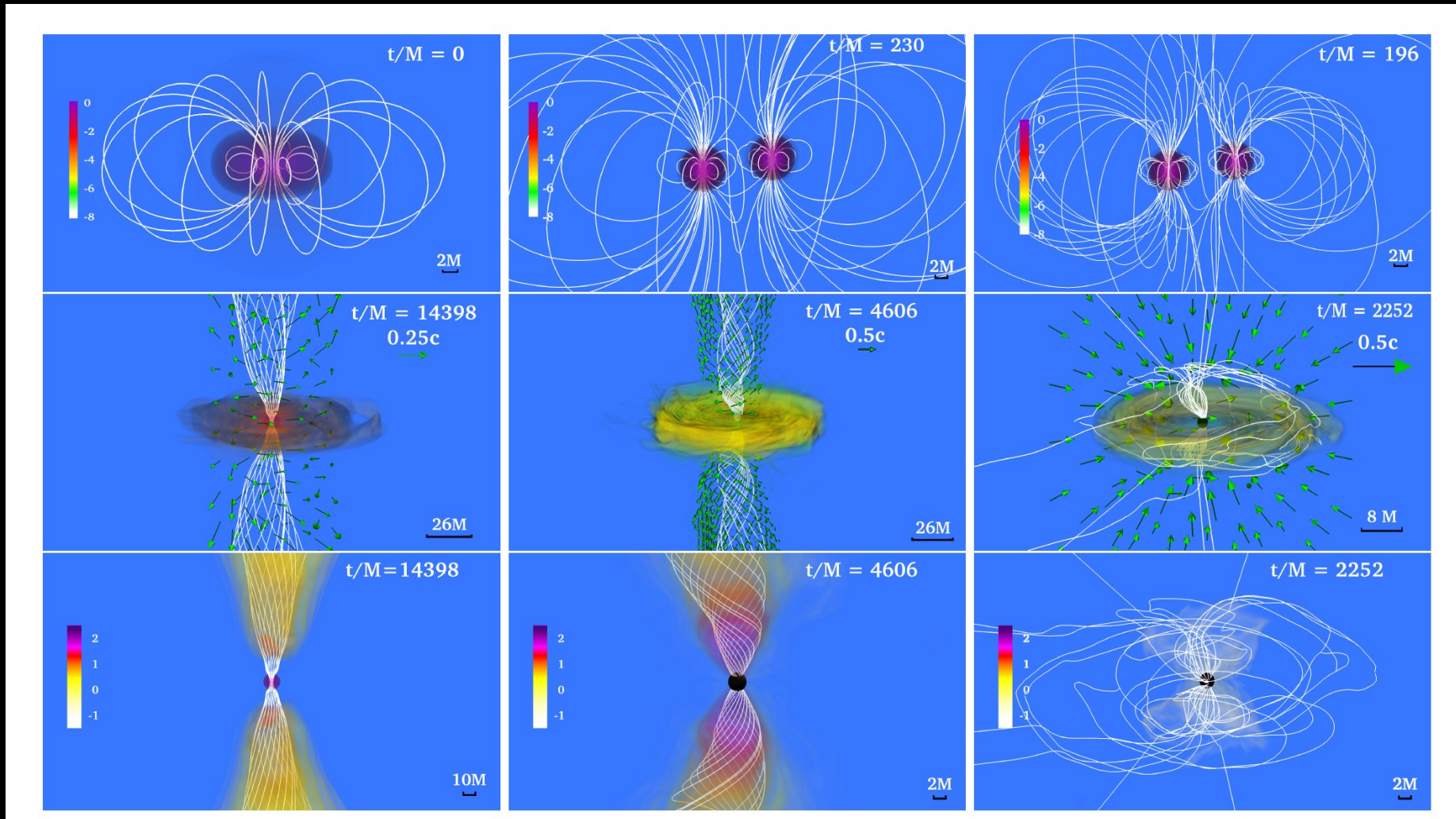
Only dynamical ejecta



Collapse behavior



- ▶ GRB-like emission may be another argument for delayed collapse in GW170817



GRMHD simulations by Ruiz et al. 2017 suggest that delayed collapse required for jet formation

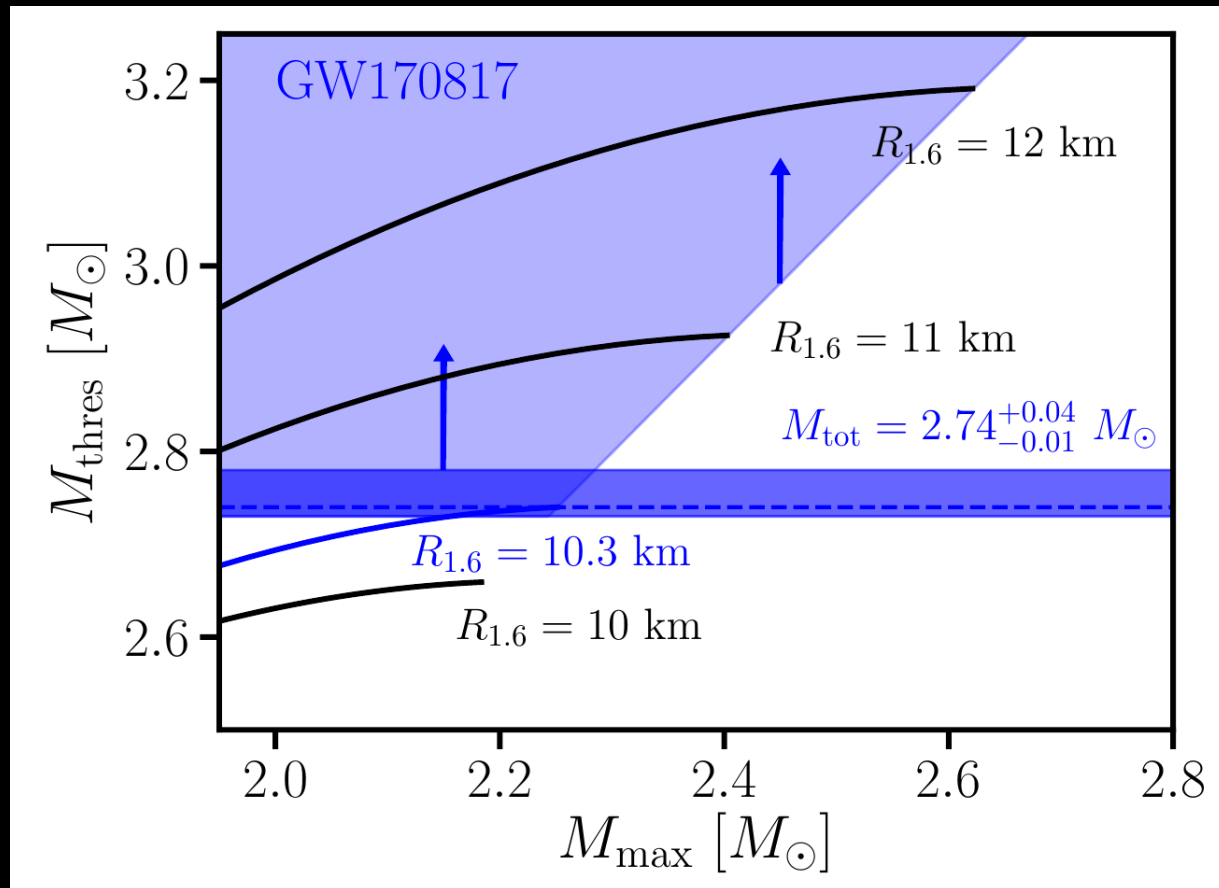
- ▶ If GW170817 was a delayed collapse:

$$M_{\text{thres}} > M_{\text{tot}}^{GW170817}$$

- ▶ Recall: empirical relation for threshold binary mass for prompt collapse:

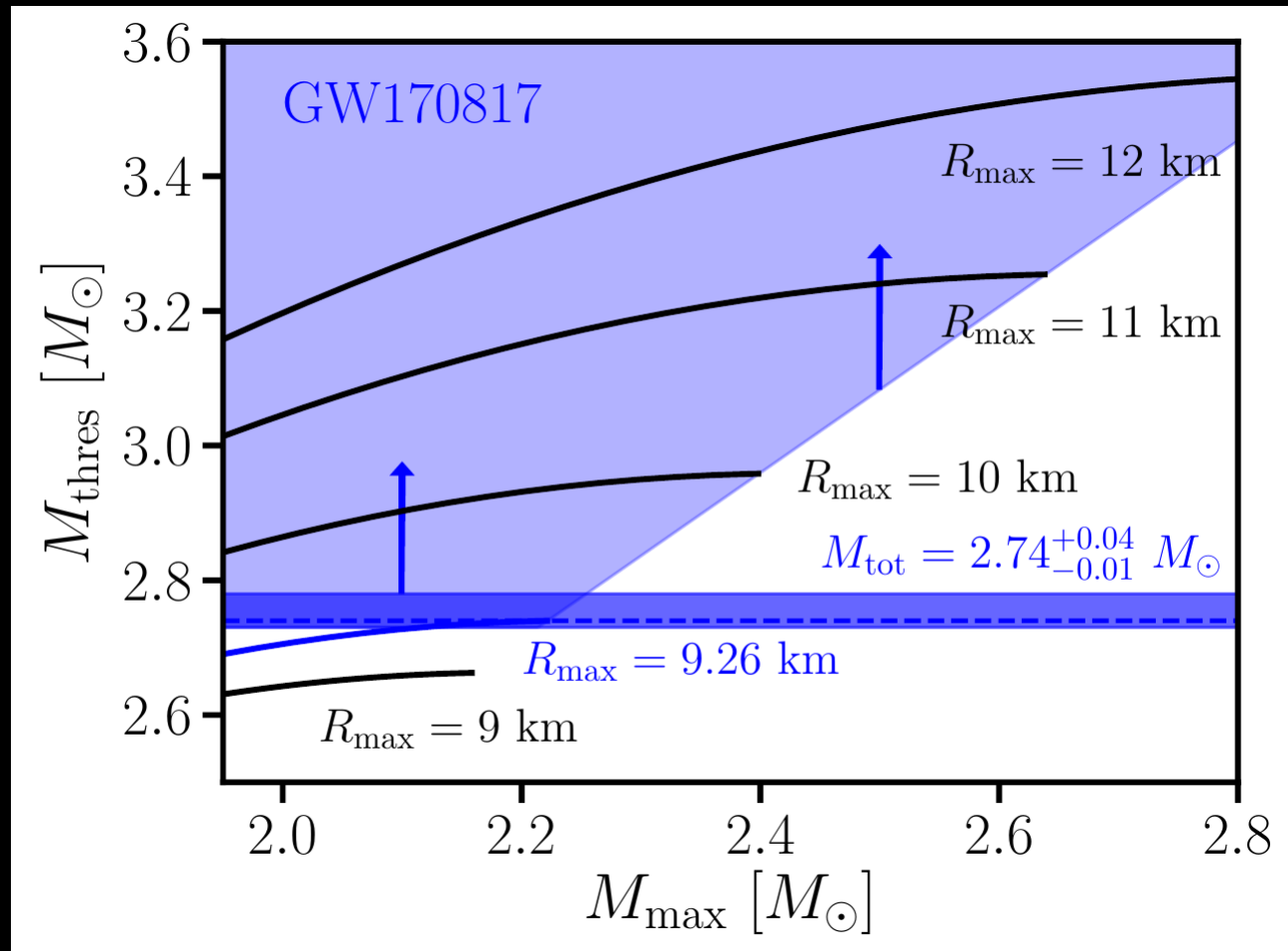
$$M_{\text{thres}} = \left(-3.6 \frac{G M_{\text{max}}}{c^2 R_{1.6}} + 2.38 \right) M_{\text{max}} > 2.74 M_{\odot} \quad \text{with } M_{\text{max}}, R_{1.6} \text{ unknown}$$

- ▶ Causality: speed of sound $v_s \leq c$



$$M_{\text{thres}} = \left(-3.6 \frac{G M_{\text{max}}}{c^2 R_{1.6}} + 2.38 \right) M_{\text{max}}$$

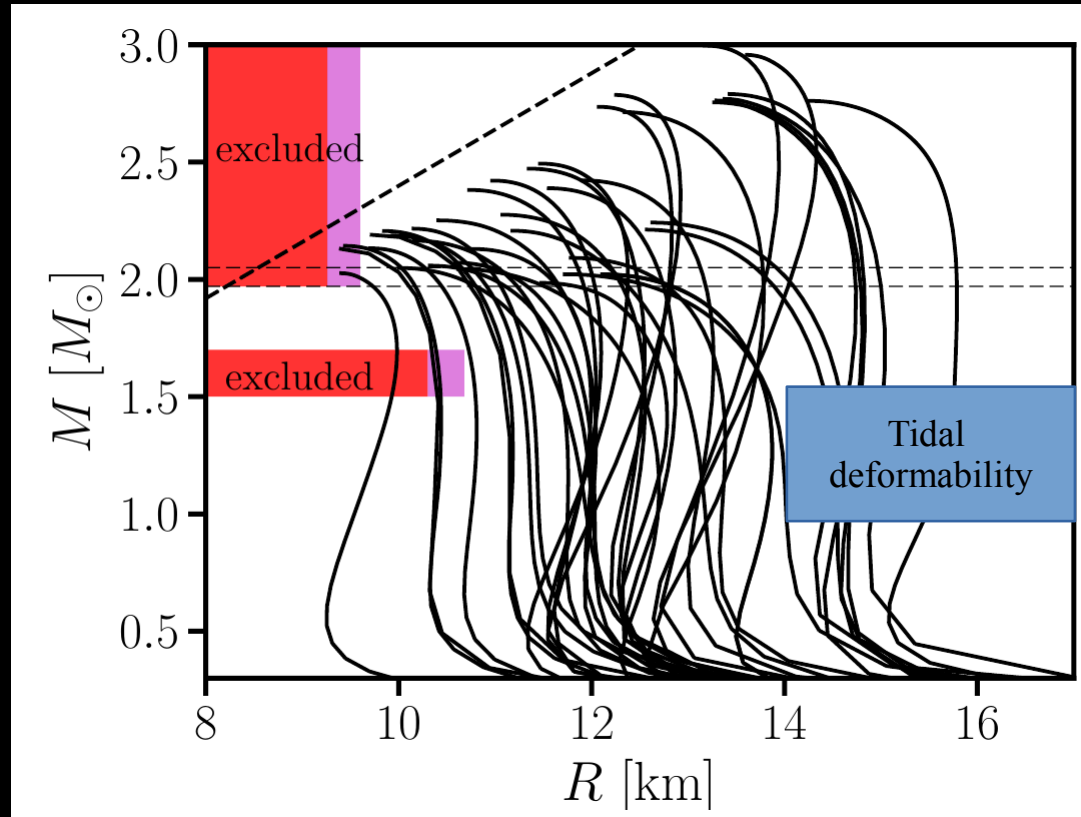
$$v_S = \sqrt{\frac{dP}{de}} \leq c \rightarrow M_{\text{max}} \leq \kappa R_{1.6} \Rightarrow M_{\text{thres}} \geq 1.2 M_{\text{max}}$$



$$M_{\text{thres}} = \left(-3.38 \frac{GM_{\text{max}}}{c^2 R_{\text{max}}} + 2.43 \right) M_{\text{max}}$$

+ causality \rightarrow $M_{\text{thres}} \geq 1.2M_{\text{max}}$

NS radius constraint from GW170817



Bauswein et al. 2017

- ▶ $R_{1.6} > 10.7$ km
- ▶ Excludes very soft nuclear matter

(Radice et al. 2018 follows similar arguments to constrain tidal deformability)

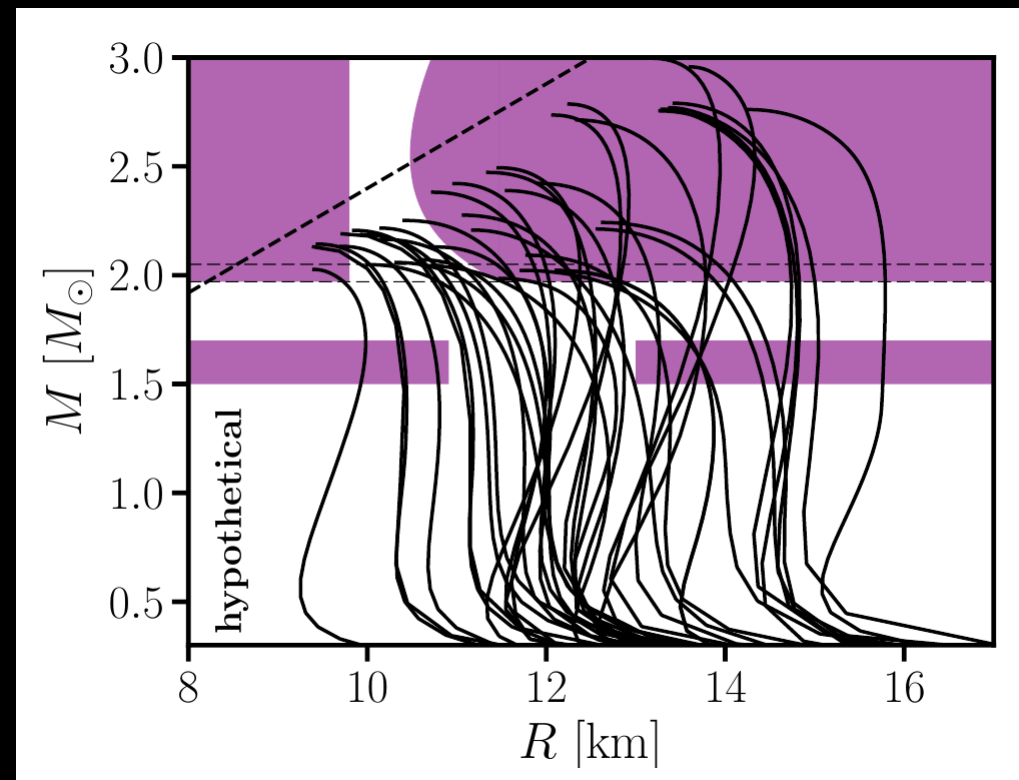
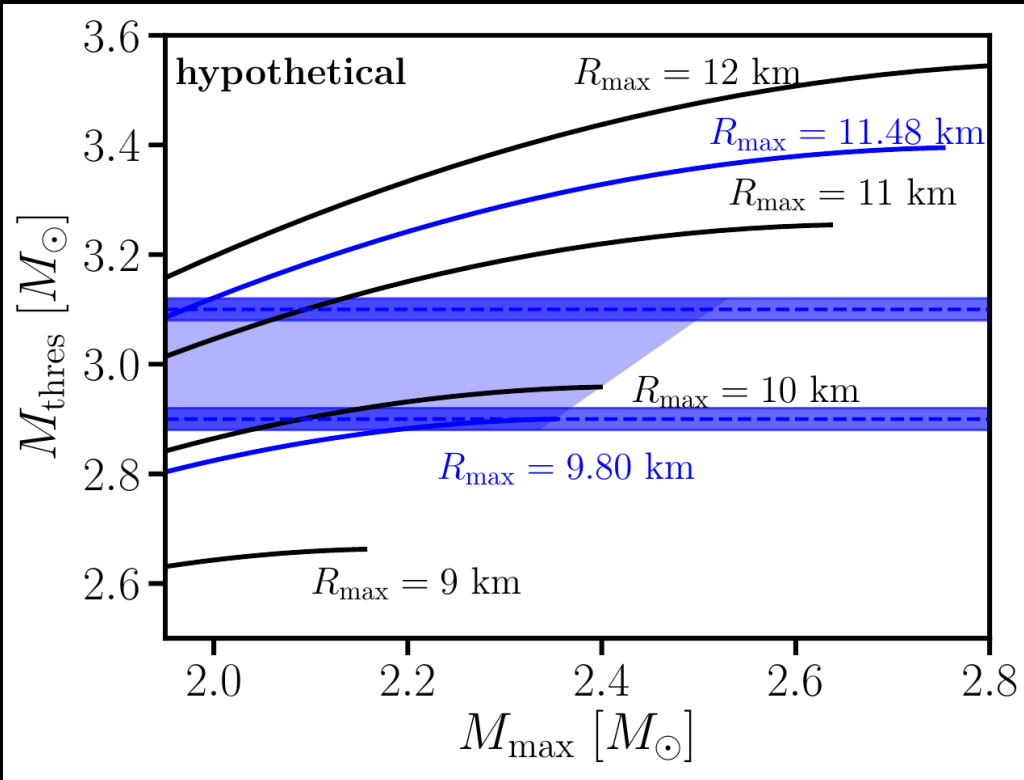
Discussion

- ▶ Binary masses well measured with high confidence error bar
- ▶ Clearly defined working hypothesis: delayed collapse
 - testable by refined emission models
 - as more events are observed more robust distinction
- ▶ Very conservative estimate, errors can be quantified
- ▶ Empirical relation can be tested by more elaborated simulations (but unlikely that MHD or neutrinos can have strong impact on M_{thres})
- ▶ Confirmed by semi-analytic collapse model
- ▶ Low-SNR constraint !!!

Future

- ▶ Any new detection can be employed if it allows distinction between prompt/delayed collapse
- ▶ Low-SNR detections sufficient !!! → that's the potential for the future
 - we don't need louder events, but more
 - complimentary to existing ideas for EoS constraints

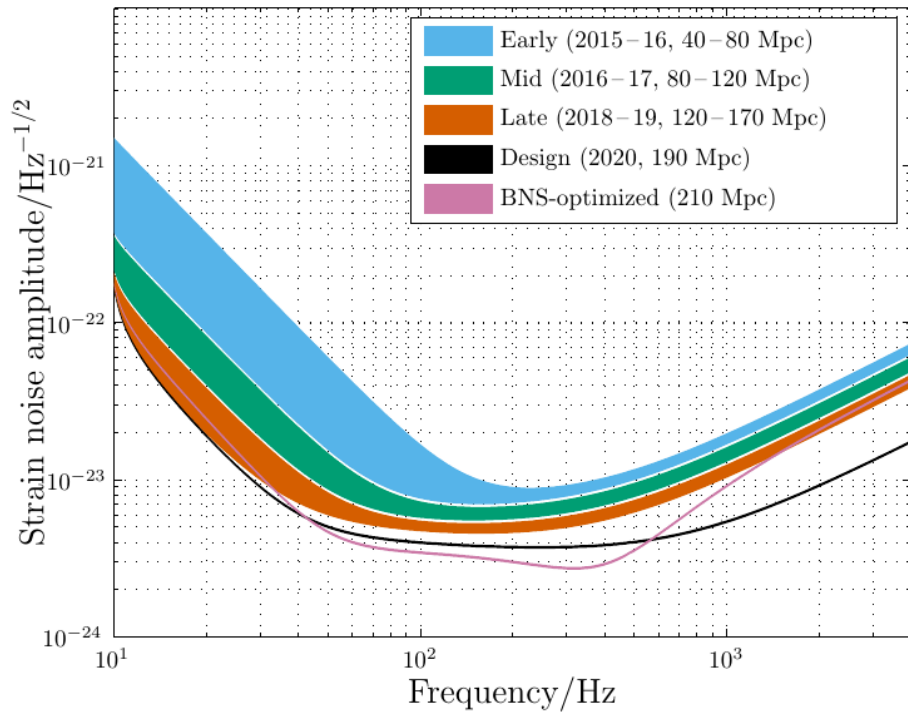
Future detections (hypothetical discussion)



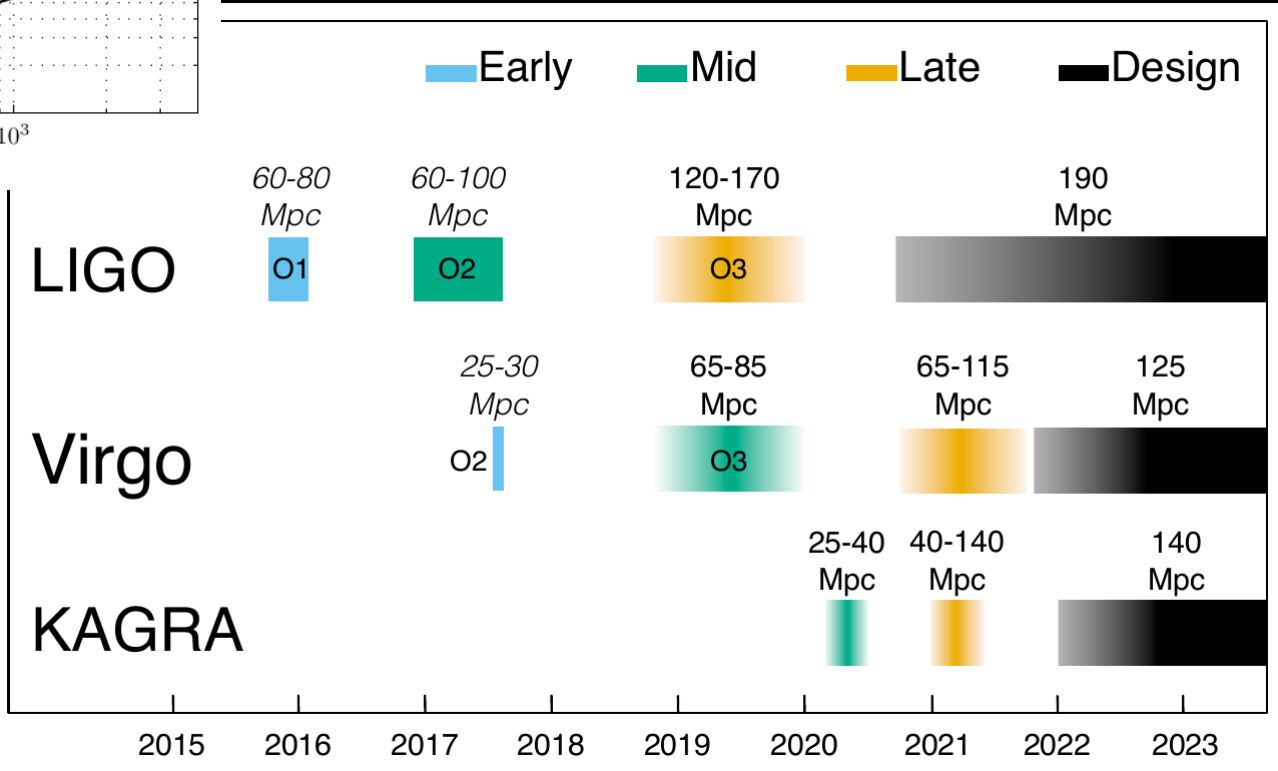
- as more events are observed, bands converge to true M_{thres}
- prompt collapse constrains M_{max} from above

Future plans

Advanced LIGO



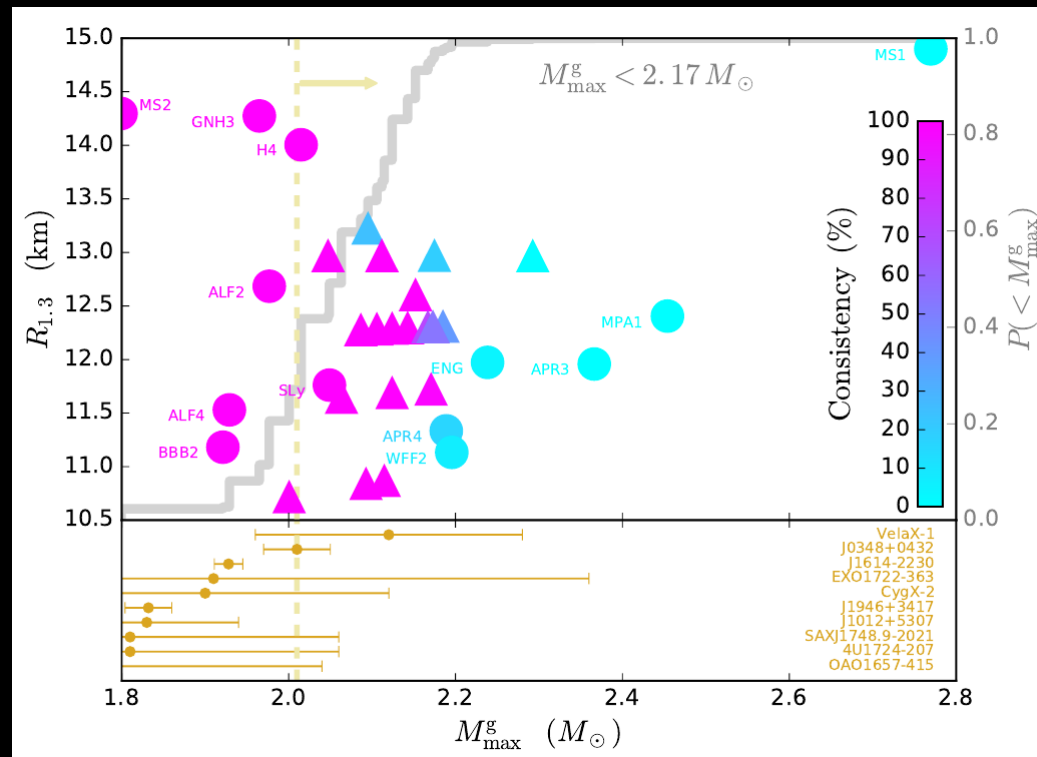
Abbott et al. 2017



Maximum mass

M_{\max} from GW170817

- ▶ Arguments: no prompt collapse; no long-lasting pulsar spin-down (too less energy deposition)
- ▶ If GW170817 did not form a supramassive NS (rigidly rotating $> M_{\max}$)
→ $M_{\max} < \sim 2.2-2.4 M_{\text{sun}}$ (relying on some assumption)



Constrain M_{\max}

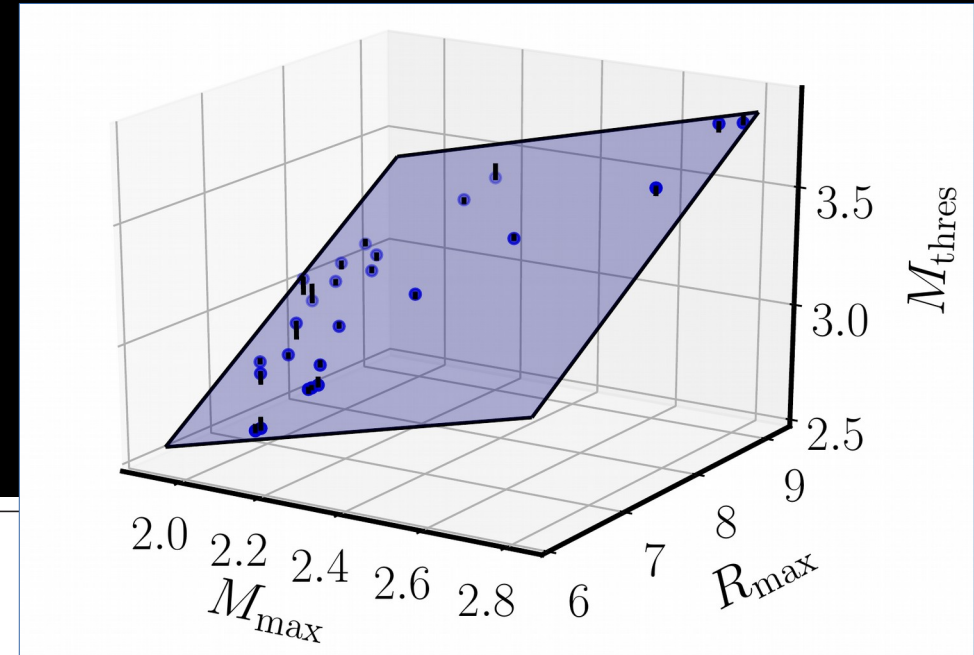
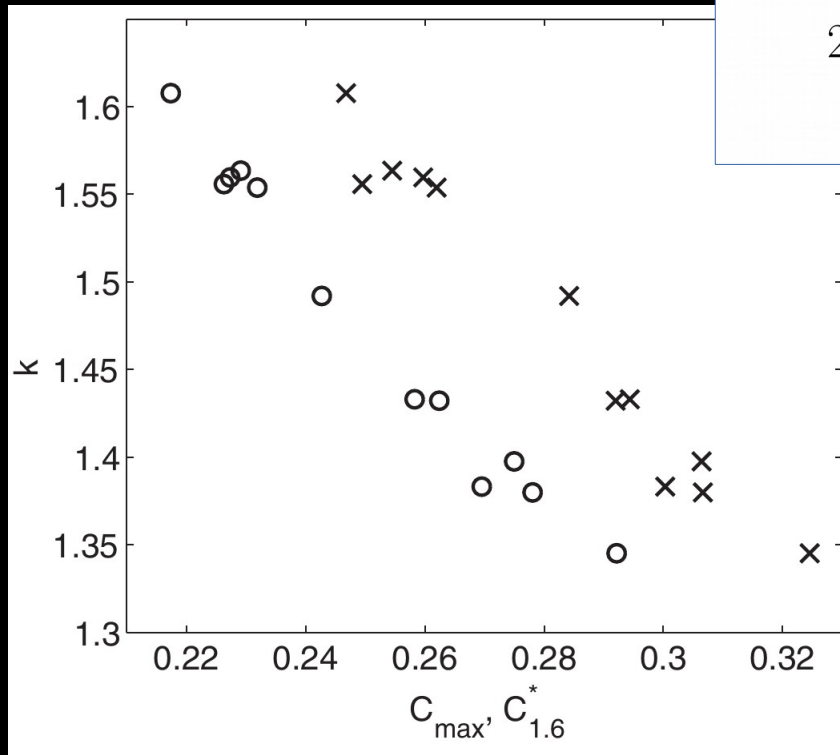
- ▶ Measure several NS mergers with different M_{tot} – check if postmerger GW emission present or through em observations

→ M_{thres} estimate

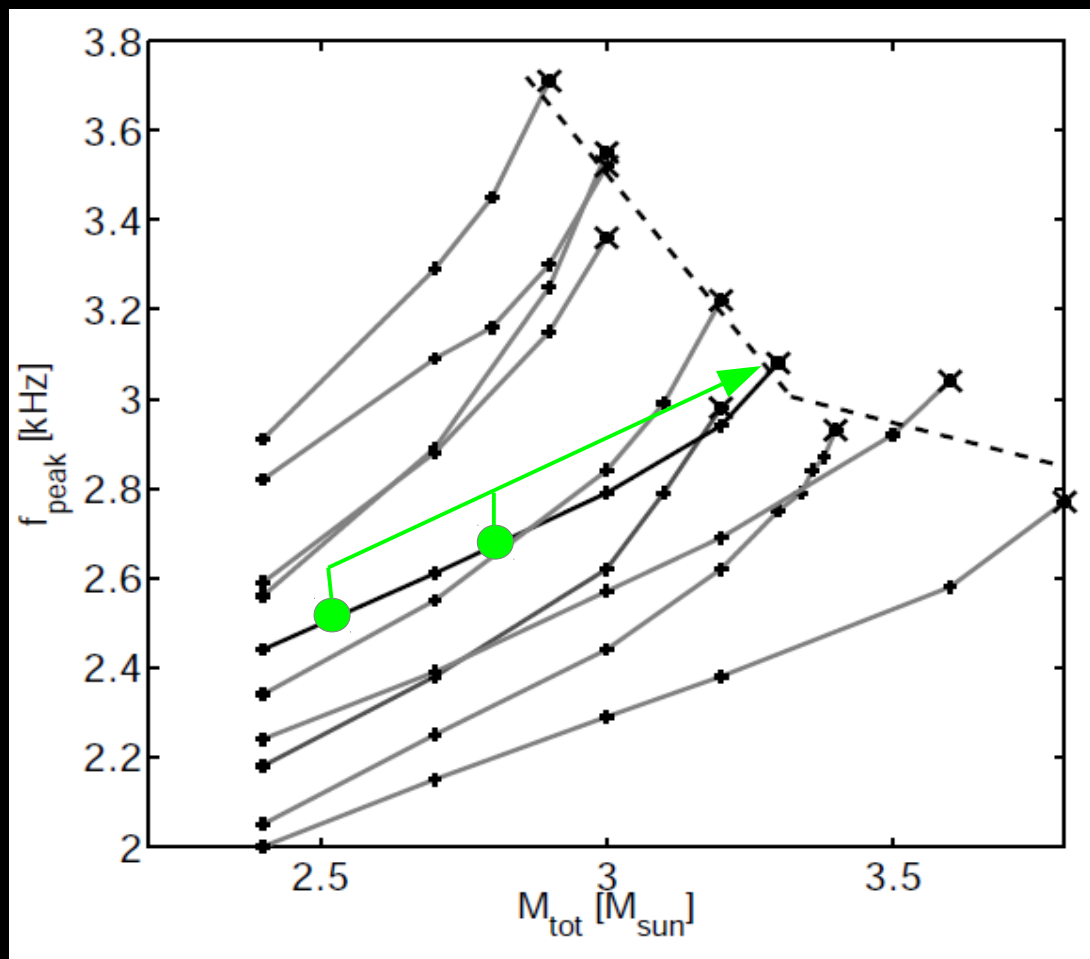
- ▶ Radius e.g. from postmerger frequency
- ▶ Invert fit

$$M_{\text{thres}} = \left(-3.6 \frac{G M_{\max}}{c^2 R_{1.6}} + 2.38 \right) M_{\max}$$

→ M_{\max}



Alternative: f_{peak} dependence on total binary mass



(every single line corresponds to a specific EoS
→ only one line can be the true EoS)

$$f_{peak} \sim \sqrt{\frac{M}{R^3}}$$

Bauswein et al. 2014

Dominant GW frequency monotone function of M_{tot}

Threshold to prompt BH collapse shows a clear dependence on M_{tot} (dashed line)

Conclusions

- ▶ GW170817 first detected NS merger (apart from earlier GRBs) → presumably high rate → promising for future detections
- ▶ Tidal deformability already constrained
→ excludes very stiff EoS
- ▶ Presumable delayed collapse in GW170817 (bright emission → high ejecta mass)
→ rules out very soft EoS ! ($R > 10.7$ km)
- ▶ Collapse behavior M_{thres} can also determine M_{max} in future (some similar tentative arguments point to $M_{\text{max}} \leq \sim 2.4 M_{\text{sun}}$)
- ▶ Dominant postmerger GW frequency scales tightly with NS radius → promising method for accurate future constraints
- ▶ long-term goal: GW asteroseismology of merger remnants